Polyphosphazenes Enable Durable, Hemocompatible, Highly Efficient Antibacterial Coatings

Victoria Albright,[1] Daniel Penarete,[2] Mary Stack,[3] Jeremy Zheng,[2] Alexander Marin[4], Hanna Hlushko,[1] Hongjun Wang,[3,5,] Arul Jayaraman,[2,6] Alexander K. Andrianov[4], and Svetlana A. Sukhishvili[1]

[1]Department of Materials Science & Engineering,
[2]Department of Biomedical Engineering, and
[6]Department of Chemical Engineering,
Texas A&M University, College Station, Texas, USA

[3]Department of Biomedical Engineering, Stevens Institute of Technology, Hoboken, NJ, USA
[4]Institute for Bioscience and Biotechnology Research, University of Maryland, Rockville, MD, USA
[5]Department of Chemistry and Chemical Biology, Stevens Institute of Technology, Hoboken, NJ, USA

Abstract:

Biocompatible antibacterial coatings are highly desirable to prevent bacterial colonization on a wide range of medical devices from hip implants to skin grafts. Traditional polyelectrolytes are unable to directly form coatings with cationic antibiotics at neutral pH and suffer from high degrees of antibiotic release upon exposure to physiological concentrations of salt. Here, novel inorganic-organic hybrid polymer coatings based on direct layer-by-layer assembly of anionic polyphosphazenes (PPzs) of various degrees of fluorination with cationic antibiotics (polymyxin B, colistin, gentamicin, and neomycin) are reported. The coatings displayed low levels of antibiotic release upon exposure to salt and pH-triggered response of controlled doses of antibiotics. Importantly, coatings remained highly surface active against *Escherichia coli* and *Staphylococcus aureus*, even after 30 days of pre-exposure to physiological conditions (bacteria-free) or after repeated bacterial challenge. Moreover, coatings displayed low (<1%) hemolytic activity for both rabbit and porcine blood. Coatings deposited on either hard (Si wafers) or soft (electrospun fiber matrices) materials were non-toxic towards fibroblasts (NIH/3T3) and displayed controllable fibroblast adhesion *via* PPz fluorination degree. Finally, coatings showed excellent antibacterial activity in *ex vivo* pig skin studies. Taken together, these results suggest a new avenue to form highly tunable, biocompatible polymer coatings for medical device surfaces.

Keywords: Fluoropolymers, polyphosphazenes, self-defensive, layer-by-layer, antibacterial, hemocompatible

Introduction:

Preventing bacterial colonization of surfaces in a controlled manner is highly desired for many biomedical devices.[1-3] Antibiotics are the most potent clinically used antibacterial agents that save millions of lives; however, their excessive use has led to a health crisis associated with the development of bacterial resistance.[4] Traditional materials physically trap antibiotics and continuously elute them, greatly contributing to this crisis by exposing bacterial strains to unnecessary, low doses of antibiotics. A viable alternative approach is to create non-eluting coatings that retain antibiotics in normal physiological conditions, and kill bacteria only upon surface colonization *via* a stimulus such as pH[5-8] or enzymes[9] specific to the bacteria-surrounding media (a scenario exploited in self-defensive coatings), or as a result of direct contact of bacteria

with the coating.[10] One attractive way to make such coatings is to use the layer-by-layer (LbL) technique,[11] which enables all-aqueous deposition of coatings of controlled nanoscopic thickness onto arbitrary substrates of a variety of shapes and chemistries.

While several self-defensive LbL coatings have been engineered,[5,6,9,12] a challenge remains to simultaneously achieve a coating that does not elute antibiotics while also maintaining hemocompatibility and cytocompatibility. Although cationic charge on antibiotics can enhance their interaction with anionic polyelectrolytes, the use of electrostatic interactions to construct antibiotic-retaining coatings using traditional synthetic poly(carboxylic acid) has been unsuccessful because of hydrophilicity of the polyacids.[13] Nevertheless gentamicin (a cationic aminoglycoside) could be temporarily trapped within nanocoatings *via* co-assembly with a poly(carboxylic acid) and poly(beta-amino esters).[14] While such coatings showed efficacy against *Staphylococcus aureus* in a rabbit bone model,[15] the antibiotic release, driven by the degradation of the polyesters, was continuous and not "on-demand". In contrast, our group recently reported self-defensive LbL films of a small polyphenol (tannic acid) and cationic antibiotics (tobramycin, gentamicin, and polymyxin B), which released antibiotics in response to bacterial colonization.[5] However, co-release of tannic acid from the coating was also observed, creating high local concentrations of tannic compounds, which can cause tissue damage[16] due to their ability to strongly bind, inhibit, and denature proteins.[17]

To resolve the antibiotic binding and the coating toxicity issues, here, we introduce a new family of self-defensive antibiotic-containing coatings built from antibiotics and water-soluble fluorinated polyphosphazenes (PPz). PPzs are a unique class of polymers with an inorganic backbone and organic side groups, which have been studied for a variety of biomedical applications.[18,19] Here, we designed PPzs with side groups from two PPzs with prior approvals. Namely, poly[bis(trifluoroethoxy)phosphazene], PTFP a hydrophobic non-biodegradable fluoropolymer, which shows outstanding hemocompatibility and is currently employed as a coating in FDA approved Cobra-PzF coronary stent[20-22] and poly[di(carboxylatophenoxy)phosphazene], PCPP, a biodegradable, ionic PPz, which is currently in phase I/II clinical trials as an injectable.[23] By combing fluorinated and ionic functionalities, water-soluble macromolecules suitable for use in LbL coatings with controlled hydrophobicity were achieved.[24,25] Moreover, such macromolecules demonstrate some unique properties, such as the ability to form stable complexes with multivalent ions and proteins in aqueous salt media

(phosphate buffered saline, PBS), in which conventional poly(carboxylic acids) fail to do so.[26-31] Importantly, the hydrolytic degradation profile of PCPP is well-established and is characterized by a relatively long half-life (150 days) with the release of a benign by-product - hydroxybenzoic acid, which is also a well-known metabolite of propyl paraben - an excipient generally regarded as safe (GRAS) by the FDA.[32,33] Therefore, fluorinated PPzs are expected to degrade so that the ionic component gradually diminishes over time with the release of GRAS excipient while the FDA approved stable PTFP coating remains on the surface.

Here, we explore a new type of coating directly assembled from antibiotics and PPzs. Specifically, we investigate the capability of ionic FPs to bind, retain, and controllably release antibiotic molecules, which have only several cationic charges. First, coatings formed *via* direct LbL deposition of cationic antibiotic (polymyxin B) with ionic PPzs of different fluorination degrees on a model silicon substrate are explored to quantify coating properties, such as antibiotic content and response to stimuli such as pH, salt, and temperature. We show that fluorination degree of PPzs can be used to efficiently modulate antibiotic content and dose of 'on-demand' delivered antibiotics as triggered by pH. Further examination of the non-leachability of the coatings and their antibacterial activity reveals that long-term retention of antibiotic and antibacterial activity is possible for up to 30 days of constant exposure to physiological mimicking conditions (pH 7.5, PBS, 37 ˚C). We then focus on hemocompatibility of the coatings – a property critically important for tissue engineering applications but rarely explored with antibacterial coatings.[34,35] Furthermore, we perform cytocompatibility studies with NIH/3T3 fibroblasts, for a systematic exploration of the effect of PPz fluorination degree on antibacterial activity, cytotoxicity, and hemolysis. Next, we examine the potential of these coatings for hard and soft tissue applications by depositing them on titanium sheet or polycaprolactone/collagen electrospun fiber matrices (ES mats). Moreover, we construct coatings with a range of cationic antibiotics (polymyxin B, colistin, gentamicin and neomycin) and show that this system is highly versatile and can be used to prevent bacterial challenges against both gram-negative and gram-positive bacteria strains. Finally, PPz + Poly B films of various fluorination degrees are constructed on ES mats and their antibacterial efficacy tested in an *ex vivo*, infected, pig skin wound model study, showing the excellent capability of these coatings in complex biological environments.

Results & Discussion

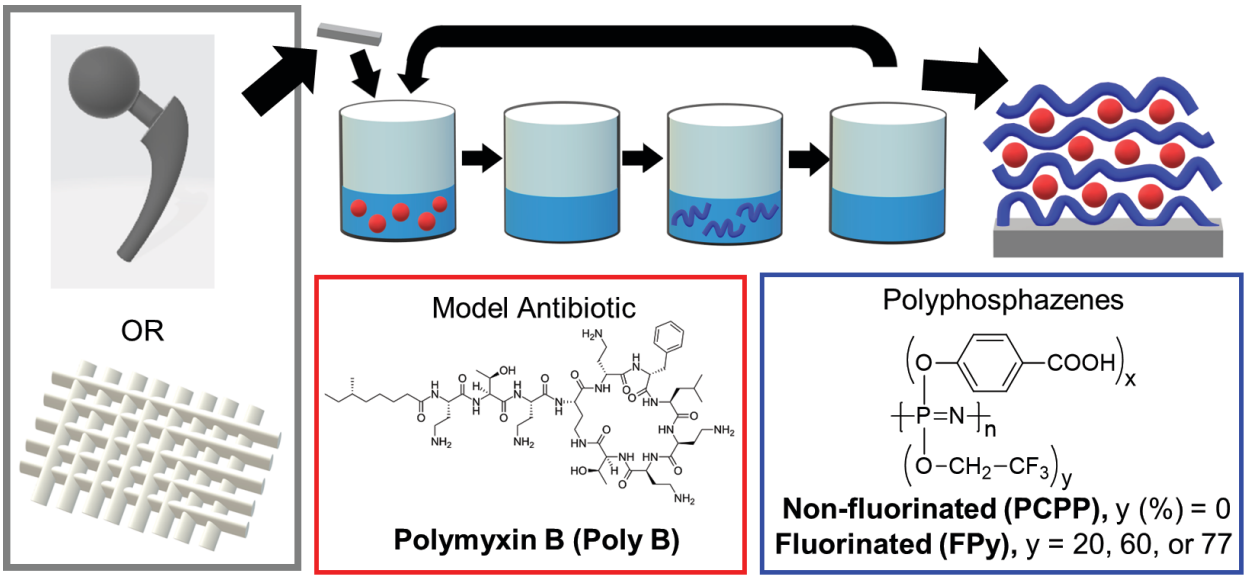

Scheme 1. Schematic representation of hip implant or wound dressing as potential substrates and layer-by-layer (LbL) assembly of antibiotics and polyphosphazenes. Chemical structures of model cationic antibiotic and various polyphosphazenes used as LbL components. LbL assembly was conducted from all aqueous solutions at pH 7.5, with a phosphate buffer (0.15 M, pH 7.5) wash in between each deposition step.

Scheme 1 illustrates the coating formation technique *via* sequential deposition of cationic antibiotics with ionic PPzs of varied fluorination degrees and shows chemical structures of a representative antibiotic, polymyxin B (Poly B), fluorinated PPzs (FPy, where y is % of fluorinated groups), and a non-fluorinated PPz, poly[di(carboxylatophenoxy)phosphazene] (PCPP). Molecular weights (Mw) of all polymers used in this study can be seen in **Table S1.** Even though fluorination is well known to increase hydrophobicity and decrease water solubility, all utilized PPzs were soluble in water, even those with fluorination degrees of 20, 60, and 77% (*i.e.* FP20, FP60, and FP77, respectively), enabling deposition of hydrophobic coatings from aqueous solutions onto hydrophilic surfaces of Si wafers. **Fig. 1A** shows ellipsometric thicknesses of dry films assembled at pH 7.5 using Poly B and PPzs with varied fluorination degrees. Interestingly, despite only a small number of charges on each antibiotic molecule, coatings could be directly assembled using all PPzs. 20 bilayers (BL) of coating resulted in film thicknesses of 120 ± 20, 103 ± 5, 150 ± 21, and 138 ± 15 nm for PCPP, FP20, FP60 and FP77 coatings with Poly B, respectively.

To ensure comparability between samples for the rest of the studies, films of matched thickness were used. This behavior is in sharp contrast to traditional polyelectrolytes (PAA, PMAA, etc.), which are unable to support LbL growth of cationic antibiotics at neutral pH (**Fig. S1A**). To understand why PPzs enable such growth while conventional polyelectrolytes are unable to, complexes in aqueous solution were studied *via* dynamic light scattering (DLS) for the three fluorinated PPzs, the non-fluorinated PPz - PCPP, and poly(acrylic acid), PAA (**SI Fig. S1B**). These results suggest that all PPzs strongly interacted with Poly B, forming molecular aggregates at Poly B concentrations, which were dramatically lower (up to 40-fold) than those needed for a conventional polyelectrolyte – PAA. Moreover, the lowest concentration of Poly B required to induce aggregation was observed for highly fluorinated PPzs, suggesting stronger binding of these polymers with antibiotics due to hydrophobic interactions.

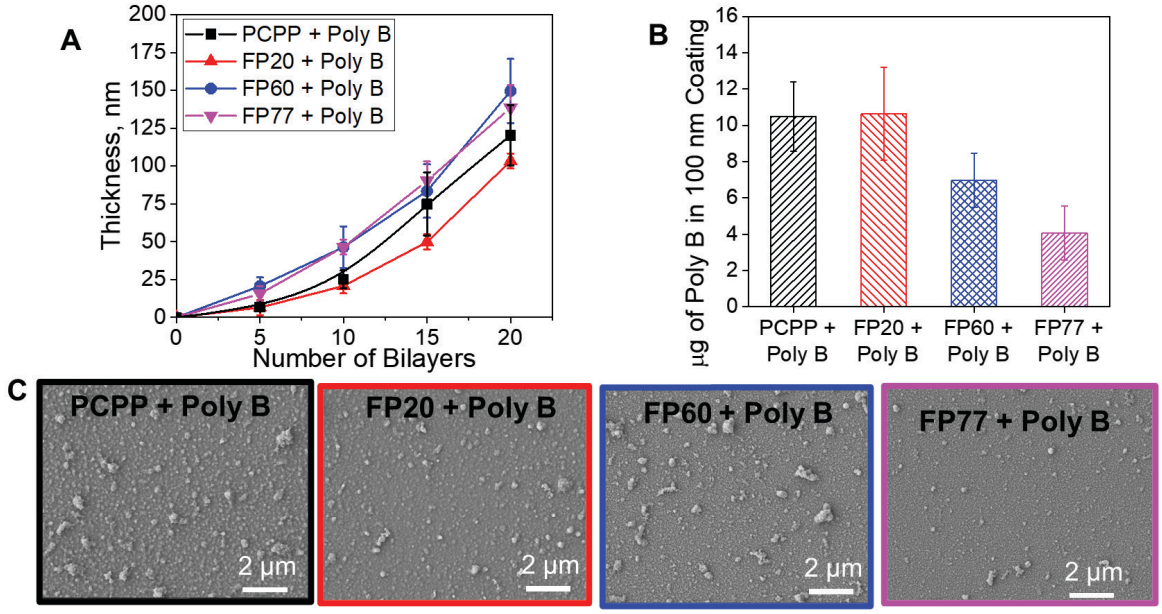

Fig. 1. (A) Dry thicknesses of LbL films as measured by spectroscopic ellipsometry for assembly of Poly B with PPzs with different fluorination degrees. (B) Micrograms of Poly B in a 100 nm film on a 1x1 cm^2 wafer as measured by LC-MS for dissolved films. (C) SEM images of 100 nm coatings of PPzs + Poly B.

To quantify the amount of Poly B retained in the LbL assemblies, coatings were dissolved in basic conditions and resulting solutions analyzed *via* liquid chromatography-mass spectrometry

(LC-MS) to determine the concentration of Poly B. LC-MS analysis of the 2+ and 3+ ions of Poly B was conducted as described in the Materials and Methods sections. Measured amounts of Poly B in the film were normalized for 100 nm films on 1 x 1 cm^2 wafers. **Fig. 1B** shows that PCPP- and FP20-based films contained approximately the same load of Poly B (10.5 ± 1.9 and 10.6 ± 2.5 μg, respectively), while the antibiotic content for FP60 and FP77 coatings of the same thickness decreased to 7.0 ± 1.5 and 4.0 ± 1.5 μg, respectively. This decrease suggests that antibiotics were bound within the film by electrostatic interactions to ionic groups in the polymer chains, and that less antibiotic was assembled with highly fluorinated PPzs because of the lower density of ionic groups in these polymers. Control studies with PCPP of various Mw confirm negligible influences of polymer molecular weight on film thickness and antibiotic content (**SI Fig. S2A&B**). Therefore, the observed results are due to differences in polymer fluorination degree. SEM studies revealed that PPz + Poly B coatings of all fluorination degrees had a similar bumpy topography (**Fig. 1C**). Such bumpy coatings are not surprising, as we have previously reported small molecule coatings (tannic acid + antibiotics) to have very bumpy morphologies.[5]

Loss of antibiotics upon exposure to salt is common for electrostatic coatings, because of the ease of disruption of their ionic pairing with polymers by physiological concentrations of ions. The data in **Fig. 2A** illustrate this point, showing that exposure to PBS at room temperature caused ~70% loss of dry film thickness of Poly B-saturated covalently crosslinked surface attached hydrogel built from non-PPz polyanions, poly(methacrylic acid) (PMAA), whose fabrication is described in our previous publications.[6] However, switching from carbon-backbone PMAA to -P=N- backbone non-fluorinated PPz (*i.e.* PCPP) not only enabled direct deposition of antibiotic-containing films as shown in **Fig. 1**, but also decreased losses of film thickness due to exposure to salt to ~20% as shown in **Fig. 2A**. An increase in fluorination degree of PPzs further decreased losses, with highly fluorinated FP60 and FP77 almost completely suppressing antibiotic dissociation from the coating in PBS at room temperature. Exposure of the coatings to PBS at 37 °C, in order to better mimic physiological conditions, resulted in additional losses of film thickness, with the largest retention of ~80% of film thickness observed for FP77. The adjustment of film thickness to new salt and temperature environments was fast **(SI Fig. S3)**, and no changes in film thickness occurred after 1 h of exposure to PBS at 37 ºC. This result is consistent with electrostatic control of ionic pairing with the film. Importantly, films remained stable for up to 30 days in physiological-mimicking conditions at pH 7.5 (**SI Figs. S3&S4**), suggesting durability for

potential biomedical applications. At the same time, water uptake by the assembled films was strongly affected by hydrophobicity of PPzs. **Fig. 2B** shows that PCPP + Poly B films swelled the most while the fluorinated films swelled less, as would be expected for polymers of increasing hydrophobicity.

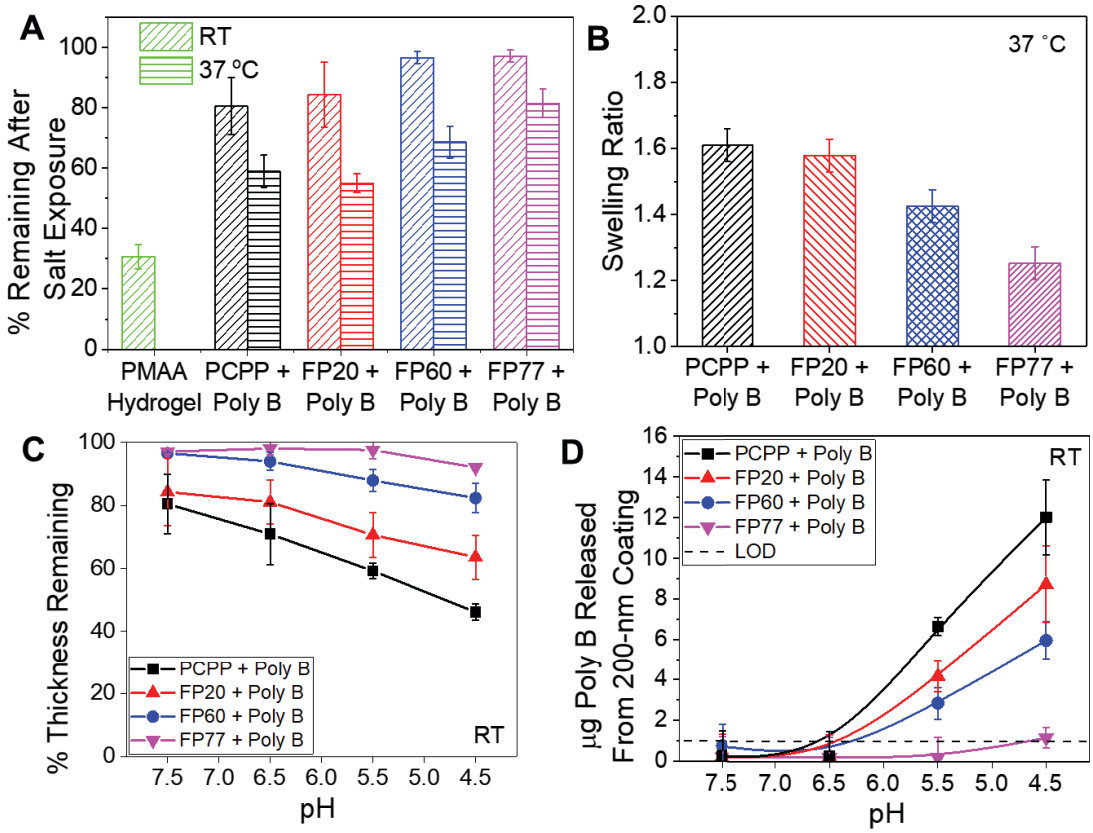

Fig. 2. (A) Remaining film thickness after exposure to physiological salt conditions (PBS, pH 7.5) at room temperature (RT) or at 37 ºC. (B) Swelling ratio of PPz + Poly B films in PBS at 37 ˚C as measured by *in situ* ellipsometry. Effect of pH on film thickness (C) and amount of antibiotic released (D) after 1 h exposure to PBS at RT. Dashed line in D represents the limit of detection.

Well-known pathogens like *Staphylococcus aureus* and *Escherichia coli* are able to acidify the medium in which they grow as a result of secretion of lactic and acetic acid, respectively.[36,37] To understand how coatings would perform under conditions similar to those of bacterial colonization, films were exposed to decreasing pHs of PBS for 1 h at RT, dried, and measured with ellipsometry while the supernatant solutions were analyzed by LC-MS for the presence of

released antibiotics. **Fig. 2C** shows that with a decrease of pH, a systematic thickness loss of the film occurred. At the same time, as film thickness decreased, more Poly B emerged in solution as measured by LC-MS (**Fig. 2D**). A similar trend was observed *via* SEM imaging in which coatings built with highly fluorinated polymers show only minimal change in topography, while coatings built with PCPP and FP20 undergo a more dramatic smoothening (**SI Fig. S5**). Importantly, all PPz + Poly B coatings released antibiotics in response to decreasing pH, and larger amounts were released at lower pHs. Unlike previous reports,[5,6] however, antibiotic dose released in this work could be controlled by the degree of PPz fluorination. Importantly, the pH-triggered release of antibiotics from coatings was pulsatile and after a pH triggered release, the coating thickness remained constant for up to 30 days, indicating no further release of antibiotics (**SI Fig. S4**).

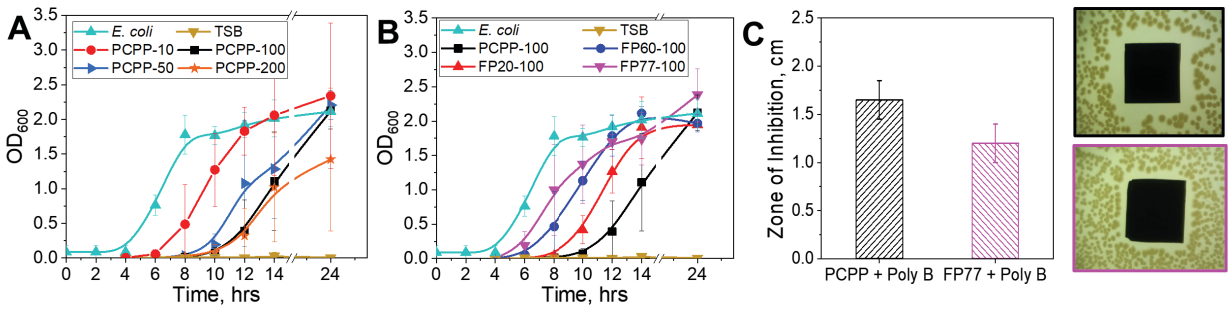

Fig. 3. Optical density of *E. coli* growing in 12 mL culture of TSB at 37 °C in the presence of PCPP + Poly B coatings of different thicknesses (A) or 100-nm coatings of various fluorination degree PPzs + Poly B (B) coatings on 1x1 cm^2 Si wafers. Starting concentration of *E. coli* was ~ 10^5 CFU/mL. All samples were run in triplicate. (C) Zones of inhibition (ZOI) of 100-nm coatings of either PCPP or FP77 with Poly B as tested with *E. coli* in duplicate. Images of ZOIs for Poly B coatings constructed using PCPP (top) or FP77 (bottom).

Antibacterial performance of coatings was then evaluated against *E. coli* ATCC 25922 in measurements of bacterial concentrations in solution (**Fig. 3**). *E. coli* is known to grow in TSB at 37 °C and display typical lag-log-stationary growth phases which can be determined by measuring the optical density (OD_{600}) of bacterial culture over time. As expected, *E. coli* reduces the culture pH over time (**SI Fig. S6A**), due to secretion of acetic acid.[6,37] *E. coli* is sensitive to sub-minimum inhibitory concentrations (MIC) of Poly B during the early stages of growth (4 to 14 h) (**SI Fig. S6B**). Therefore, this technique provides a convenient way to detect release of Poly B from

coatings in low concentrations. This assay (**Fig. 3**), in which large volume, exceedingly high bacterial counts, and short time periods are used, does not mimic a situation in the body but can aid in fundamental understanding of coating performance. To quantify release of Poly B from coatings, coatings were exposed to a large volume of TSB to ensure that released amount of antibiotic would not exceed MIC. MIC of *E. coli* ATCC 25922 was determined in this work as 2, 2, and 4 μg/mL for 10^3, 10^5, and 10^7 CFU/mL bacterial concentrations, respectively (**SI Fig. S7A**), which are similar to previously reported values.[38] As controls, prime layers (a monolayer of BPEI plus a monolayer of a PPz) were exposed to *E. coli*, with no appreciable difference observed in the bacterial growth (**SI Fig. S7B**), in agreement with mild antibacterial activity reported for PPzs.[39,40]

The capability of the coatings to release antibiotics and thus inhibit bacterial growth in solution was then explored with coatings of various thicknesses (10, 50, 100, and 200 nm) constructed using Poly B and PPzs with different fluorination degrees (PCPP, FP20, FP60, FP77). These coatings, abbreviated as PCPP-x or FPy-x, where x is film thickness in nanometers, were exposed to a starting concentration of ~10^5 CFU/mL of *E. coli*. **Fig. 3A** shows as soon as *E. coli* is grown in the presence of coatings as thin as 10 nm, the length of time needed to reach the log phase increased, demonstrating the release of antimicrobials into solution from the coating. Moreover, by increasing the thickness of the coating, a longer time-period was required for bacteria to reach the log phase growth. This result mimics growth curves observed for increasing antibiotic concentration in solution (**Fig. S6B**), and therefore, indicates that thicker LbL coatings release more antibiotics from the bulk of the film when triggered by bacteria-growth-induced pH decrease than thinner coatings do. Importantly, a control experiment in which PCPP + Poly B coatings were pre-exposed to pH 7.5 PBS for 1 h prior to antibacterial testing showed no difference in antibacterial performance (**SI Fig. S8**), illustrating that pH-induced antibiotic release was not affected by pre-exposure to 0.15 M salt concentration. Comparing coatings of the same thickness (100 nm) but different PPz fluorination degrees reveals that the amount of antibiotic released was smaller for films built from highly fluorinated PPzs **(Fig. 3B)**. This trend is primarily due to the overall different content of antibiotics in the films. **SI Fig. S9A-C** shows that the dose of antibiotic released can be tuned for all fluorination degree PPzs by changing coating thickness, with increasing coating thickness releasing more antibiotic content.

After understanding release mechanisms of antibiotics from the coatings into solution, surface activity of PPz + Poly B coatings was assessed. Bacteria-triggered elution of antibiotics

out of the coatings was demonstrated in zone of inhibition (ZOI) assays, which were conducted with 100-nm coatings built with non-fluorinated PCPP and highly fluorinated FP77 polymers (**Fig. 3C).** Although quantification of Poly B doses can be difficult because of its slow diffusion through agar plates,[38] both PCPP-based and FP77-based coatings eluted antibiotics when challenged by bacteria. In agreement with **Fig. 3B,** more antibiotics were released from PCPP-based coatings, which contained larger initial Poly B loads (**Fig. 2B**).

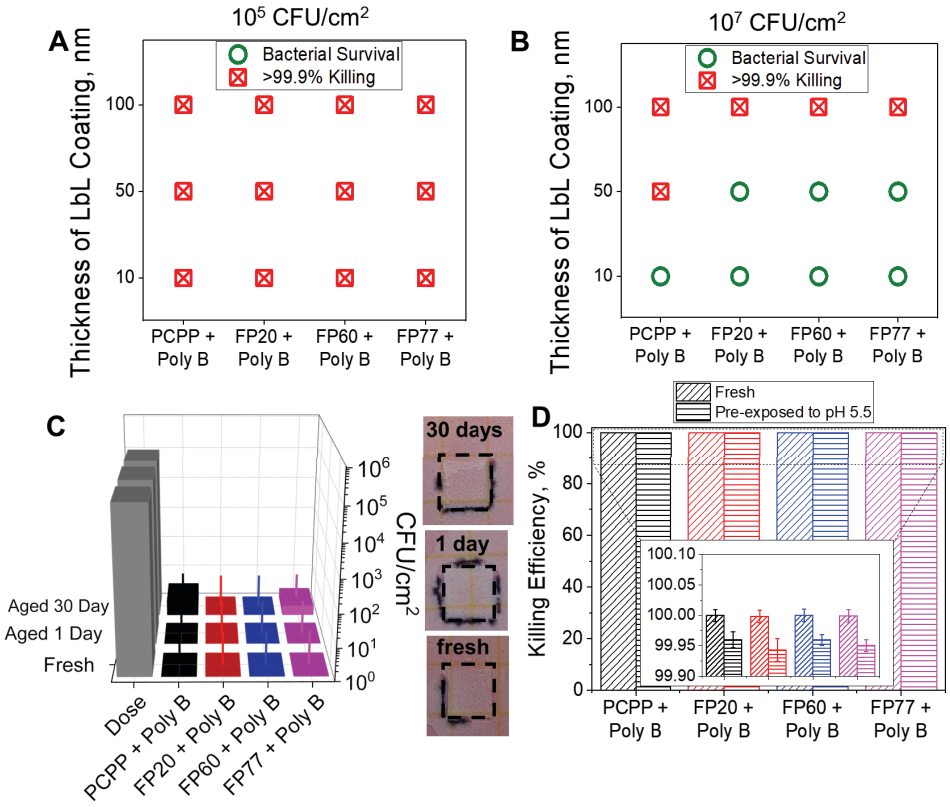

Fig. 4. Petrifilm™ assay results demonstrating the effect of coating thickness and composition on bacterial death or survival. Assay run with 10^5 (A) or 10^7 (B) CFU of *E. coli* on 1x1 cm^2 Si wafer with PPz + Poly B coatings of a variety of thicknesses and incubated for 24 h at 37˚C on a 3M™ Petrifilm™ *E. coli* Count Plate. (C) Petrifilm™ assay results demonstrating the effect of sample aging in pH 7.5 PBS at 37 ˚C on antibacterial efficacy over time, along with images of Petrifilm plates representing bacterial growth on fresh and aged coatings. Assay run with 10^5 CFU of *E. coli* on 100-nm coatings. (D) Petrifilm™ assay results for 100 nm PPz + Poly B coatings fresh or after 1 h pre-exposure to pH 5.5 PBS at 37°C challenged with 10^5 CFU of *E. coli* per sample.

To explore capability of the coatings to kill bacteria in the immediate proximity of the coated substrate, extremely high concentrations of bacteria were then directly applied to the coating surface. Specifically, a small droplet (5 μl) of *E. coli* at the desired concentration was placed on top of a 1x1 cm^2 Si wafer and incubated for 24 h at 37˚C on a 3M™ Petrifilm™ *E. coli* Count Plate. Coatings of three different thicknesses (10, 50, and 100 nm) and four different fluorination degrees (PCPP, FP20, FP60, and FP77) were tested for comparison in duplicate. The results of the assay are shown in **Fig. 4.** All coatings could prevent the growth of 10^5 CFU bacterial challenge per sample (**Fig. 4A**). However, for a 10^7 CFU per sample bacterial challenge, thicker 100-nm coatings were able to prevent growth, while 10-nm coatings failed (**Fig. 4B**). For 50 nm coatings, only PCPP-based coatings, which had higher content of Poly B, were able to prevent bacterial growth, while the other PPz coatings failed to do so. These results illustrate high efficiency of the coatings to kill approaching bacteria and show that such efficiency can be tuned by both fluorination degree of PPzs and/or thickness of antibiotic-containing coatings.

One important property that cannot be achieved with traditional antibiotic-elution coatings is long-term potency; such coatings continuously elute antimicrobials and with time become depleted of their cargo. However, the antibiotic release mechanism in our coatings is different and involves highly localized pH-triggered release to bacteria in the vicinity of the surface. In this mode of action, even low released doses remain efficient, locally achieving MICs for thin coatings. As shown above in **Fig. 2**, self-defensive coatings retained their antimicrobial loads in the absence of bacteria when exposed to PBS at pH 7.5, thus preserving their capability of responding to bacterial attack. To understand the long-term efficacy of coatings, 100 nm PPz + Poly B coatings were aged in pH 7.5 PBS at 37 °C for 1 day or 30 days and then challenged with a bacterial dose of 10^5 CFU per sample. Remarkably, all coatings, even those soaked for 30 days in physiological conditions, were able to completely withstand a bacterial challenge of 10^5 CFU (**Fig. 4C**). These results imply that PPz + Poly B coatings can survive in the body for long periods of time and still be active. However, partial depletion of a coating can occur after primary contact with approaching bacteria due to localized acidification. Therefore, it was important to explore whether self-defensive coatings can preserve their on-demand release capability after pre-exposure to a low-acidity environment. To that end, PPz + Poly B coatings were first pre-exposed to bacteria-free pH 5.5 PBS at 37 °C for 1 h and then challenged with a bacterial dose of 10^5 CFU per sample. As illustrated in **Fig. 4D**, all coatings were able to prevent bacterial attack to nearly the same level as

fresh coatings. Such a robust antibacterial performance of the coating under these harsh testing conditions means that in spite of partial release of antibiotics in the pre-exposure buffer at pH 5.5, a significant amount of antimicrobials is retained in the coatings (see **Fig. 2**) that is sufficient to support antibacterial attack. Taken together, these results show that PPz + Poly B antibacterial coatings can endure long periods of exposure to bacteria-free environments, which mimic those in the body, and are also likely to be efficient in preventing multiple attempts of bacteria to colonize the surface.

We next addressed an important, yet often disregarded, aspect of antibacterial coatings – their interaction with blood. This scenario is common occurs upon implantation of biomaterials into the body, yet blood compatibility of materials is rarely considered at the early steps of biomaterials development. To explore hemocompatibility, coatings of Poly B with PCPP of different thicknesses (10, 50 or 100 nm), as well as coatings of Poly B with FPys with different fluorination degrees but matched thickness (100 nm) were assembled. This series of coatings enabled us to distinguish between the influences of Poly B content, film thickness, and effect of fluorination degree. In addition, solution cast films of a fluorinated PPz, poly[bis(trifluoroethoxyphosphazene)], PTFEP were used as controls. Excellent hemocompatibility of PTFEP has been clinically validated in two US Food and Drug Administration (FDA) approved products – coronary stents and embolic microbeads.[20-22] Two well-established hemolytic activity tests were employed (**Fig. 5A**) – one using whole rabbit blood,[25,41] and another using porcine red blood cells.[42-45] The results of both studies demonstrated exceptionally low hemolytic activity of all coatings (less than 1%) regardless of degree of fluorination of PPzs **(Fig. 5A**) and thickness of the coating (**SI Fig. S10A**). In solution, all PPz polymers showed no hemolytic activity (less than 0.1%) (**SI Fig. S10B),** while Poly B exhibited concentration-dependent hemolysis with a maximum hemolysis degree of 2% reached for an antibiotic concentration of 10 μg/mL (**SI Fig. S10C**). Therefore, the fact that PPz-containing coatings, regardless of their overall content of antibiotics (determined by PPz type and film thickness), demonstrated very low hemolysis degrees implies that Poly B is screened from direct interaction with blood cells by its assembly in the coatings. Importantly, the hemocompatibility of all Poly B-containing coatings was at least at the same level as that of PTFEP – a material with well-established performance both in animal experiments and clinical trials. [20,46-49]

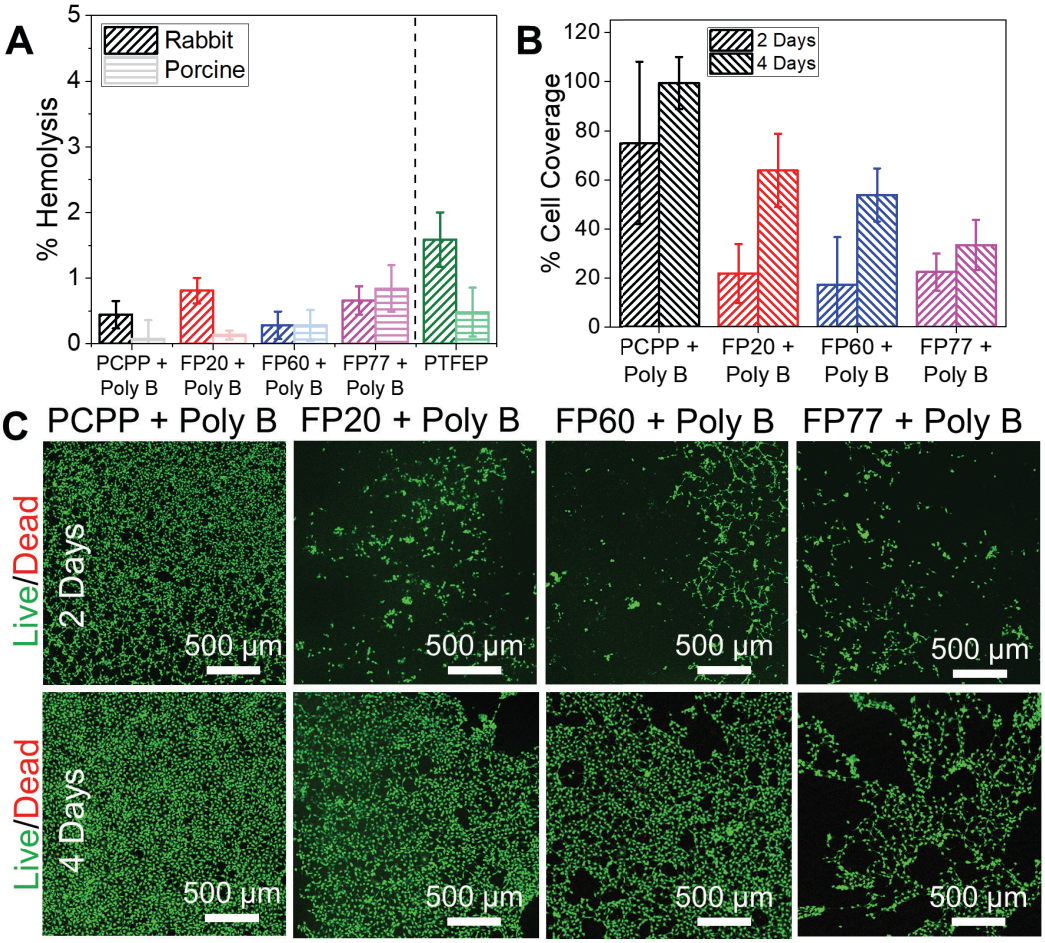

Fig. 5. (A) Hemocompatibility studies of 100 nm PPz + Poly B coatings using whole rabbit blood and porcine red blood cells. (B) Percentage surface area and live/dead staining (C) of 100 nm PPz + Poly B coatings covered with NIH/3T3 fibroblast cells after 2 or 4 days of incubation.

Furthermore, cytocompatibility of PPz + Poly B coatings, an important aspect of any biomaterial, was assessed *via* MTT assay for components in solution and live/dead staining as well as MTT assay for coatings on Si wafers using NIH/3T3 fibroblasts. Fibroblasts were exposed to different concentrations of polymers on extreme ends of fluorination degree (PCPP and FP77) as well as Poly B in solution (**SI Fig. S11A**) for 24 hours. Poly B showed negligible toxicity in all concentrations tested (0.8-100 µg/mL), while PCPP caused a distinct drop in cellular metabolism at all concentration ranges, which was significant even at the lowest concentration of 0.8 µg/mL.

This behavior was previously observed with anionic hydrogels and ascribed to the presence of ionic groups in the polymer chains.[50] Unlike PCPP, FP77 did not cause a decrease in cellular activity until a concentration of 6.3 μg/mL. Assuming the worst case scenario that an entire 100 nm film on a 1 x 1 cm^2 substrate dissolved (and matched polymer densities for ease of calculation), solution concentrations for a PCPP + Poly B film would roughly be 5 μg/mL of Poly B and 7.5 μg/mL of PCPP, while for a FP77 + Poly B film, roughly 2 μg/mL of Poly B and 11μg/mL of FP77 would be released. At the tested concentrations closest to these concentrations, PCPP at 6.25 μg/mL has a viability of 64 ± 10% or FP77 at 12.5 μg/mL has a viability of 81 ± 8%. These results suggest that fluorinated PPzs are less likely than their non-fluorinated counterparts to cause an extreme decrease in cellular metabolism. It is important to note however, that several reports have shown that once ionic polymers are bound in pairs in a coating, their toxicity is mitigated and therefore, behavior of fibroblasts on coatings may differ.

Next, live/dead staining of fibroblasts adhered to PPz + Poly B coatings of matched thickness and different fluorination degrees was performed after 2 and 4 days of incubation (**Fig. 5B&C)**. After 2 days of culture, all fluorinated coatings had fewer cells adhered compared to coatings built with PCPP. Even though PCPP was demonstrated to be more toxic to fibroblasts at a lower concentration in solution than FP77 (**SI Fig. S11**), no dead (red) cells were observed on any PPz + Antibiotics (Abx)-coated surfaces. It is possible that dead cells did not adhere well to the surface, especially since most of these surfaces are so hydrophobic. However, we were able to validate that our dead staining procedure (see SI Fig. S12) and therefore, believe that all coatings were nontoxic. At the same time, higher live cell coverage was found on PPz coatings with lower fluorination degrees. Cell coverage is dependent on many factors including cell adhesion, toxicity, and proliferative capacity. In this case, such differences can most likely be attributed to coating hydrophobicity and roughness, as such factors heavily influence the behavior of 3T3 fibroblasts.[51] To rule out that these results were caused by differences in Poly B content in the coatings, two control samples of a layer of priming agent (BPEI) and a monolayer of either PCPP or FP77 were deposited and used for fibroblast culture. **SI Fig. S11B** shows that two control monolayers exhibited drastically different cellular coverage, suggesting that the differences in cellular coverage were caused by PPz fluorination degree and not Poly B content. Importantly, after 4 days of culturing, all coatings showed increased cell coverage, suggesting that fibroblasts were able to proliferate on the samples. Importantly, few, if any, dead cells were observed on the coatings,

suggesting that all PPz + Poly B coatings were nontoxic to fibroblasts. These results are further corroborated with an MTT assay conducted on fibroblasts after 2, 4, or 6 days of incubation on top of 100 nm PPz + Poly B coatings (**SI Fig. S11C**) and controls (a priming layer of BPEI or a layer of BPEI + PCPP or FP77, as well as PCPP + Poly B coatings of three different thicknesses, **SI Fig. S11D)**. All samples showed increasing OD_{540} over time, indicating an increase in cellular metabolism for matched thickness films with PPzs of different fluorination degrees (**SI Fig. S11C**) as well as for films of different thicknesses made with one PPz (PCPP) (**SI Fig. S11D**).

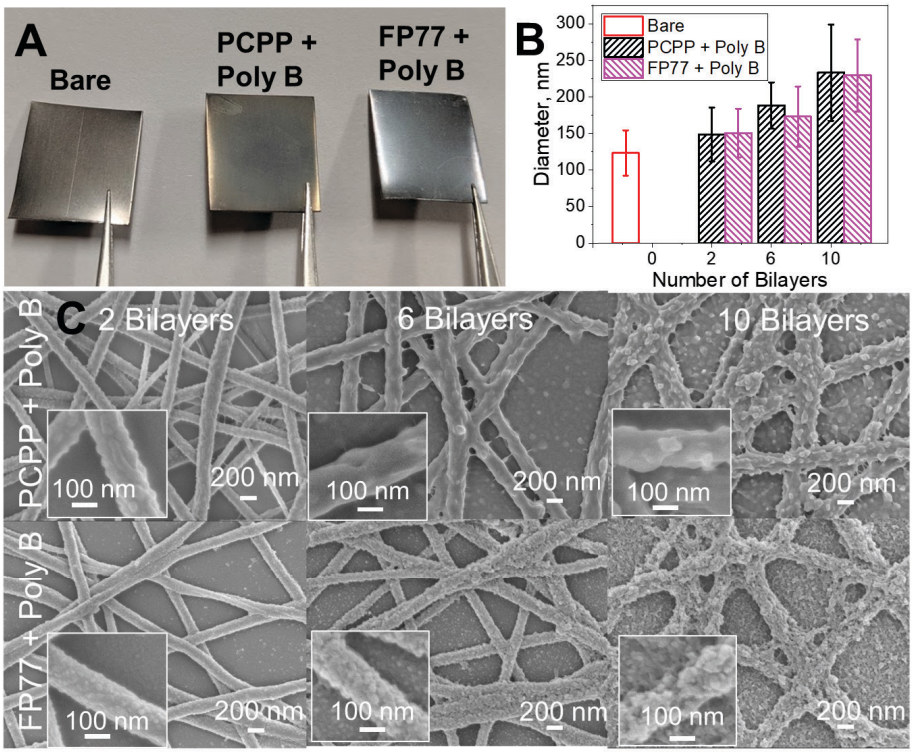

Fig. 6. (A) Images of titanium sheet bare and coated with 20 bilayers (BL) of PPzs + Poly B. Diameters (B) and (C) SEM images of 2, 6, or 10 BL PPz + Poly B coatings on polycaprolactone/collagen electrospun fiber matrices (ES mats).

The preceding studies served as a fundamental exploration of the novel coatings' general properties on a model substrate (Si wafer). Moving towards potential biomedical applications of these antibacterial coatings, we next studied various biological effects of the coatings on more physiologically relevant substrates: titanium as a hard tissue implant model and polycaprolactone/collagen electrospun fiber matrices (ES mats) as a soft tissue graft model. For loading-bearing implants such as hip implants, hard materials like stainless steel or titanium alloys

are commonly used.[52] Therefore, antibiotic-containing coatings were deposited on titanium plates (**Fig. 6A**). Importantly, coatings of all fluorination degrees were able to deposit successfully and had similar antibacterial efficacy (**SI Fig. S13**) to the coatings on Si wafers (**Fig. 4**). Specifically, 20 BL coatings of PCPP + Poly B and FP77 + Poly B on titanium plates (estimated to be roughly 100 to 150 nm based on coating thickness on Si wafers) were able to fully prevent the growth of 10^5 CFU/cm^2 *E. coli* and almost fully prevent the challenge of 10^7 CFU/cm^2 (< 60 *E. coli* survived). This result is not surprising since both silicon wafers and titanium plates are two-dimensional, hard materials and therefore, coating properties are not expected to be very different.

In contrast, differences in the coating performance, with regard to both bacterial and mammalian cells, were expected when the coatings were deposited on softer and/or three-dimensional materials, such as those commonly used in soft tissue implants and wound dressings. Electrospun fiber matrices comprised of nano- and/or micro-scale fibers provide high interconnected porosity, which effectively mimics the native extracellular matrix,[53] making them promising wound dressing materials. Additionally, previous studies, by our group[54] and others,[55] have shown that electrospun fiber matrices are excellent substrates for LbL deposition. To that end, PCL/collagen fibers were electrospun onto glass coverslips resulting in fibers with an average diamater of 123 ± 31 nm **(Fig. 6B)**. Deposition of PCPP + Poly B and FP77 + Poly B onto fibers results in increasing fiber diameters (**Fig. 6B**) with coating thicknesses twice thicker than those deposited on Si wafers. Importantly, coatings well conformed to individual fibers in ES mats, with clear bumps on individual fibers, giving a similar coating topography to those on flat substrates. Depositing 2 or 6 BLs (~ 26 or 58 nm based on diameter changes (**Fig. 6B)**), preserved the open structure of fiber mats, while deposition of 10 BLs (~ 108 nm) of coating induced bridging between individual fibers. To avoid coating bridging, coatings of 6 BLs of all four PPzs were chosen to examine coating antibacterial performance and cytocompatibility. Importantly, 6 BL PPz + Poly B coatings could be deposited on fibers regardless of PPz fluorination degree (**Fig. 7A**).

Because of the large surface-to-volume ratio of ES mats, higher local concentrations of antibiotics were expected during bacteria-triggered release from coatings on fibers than from coatings on flat substrates. As proof-of-concept, PCPP + Poly B coatings of 2, 6, and 10 BLs were deposited on an extra-thick batch of ES mat (to avoid LOD problems with LC-MS), dissolved, and solution concentrations of Poly B measured with LC-MS. **SI Fig. S14A** shows that the amount of Poly B released from the coating increased with number of deposited BLs. Importantly, a coating

of just 2 BL of PCPP + Poly B on ES mats resulted in ~ 7 ± 2 μg of Poly B being released, an amount comparable to a 100 nm coating on Si wafer, which required deposition of ~15 BLs of the film. Because of this significant surface area advantage of ES mats, thinner, 6-BL coatings could be used for all antibacterial without a sacrifice in coating performance. Deposition of thinner coatings on the fibers also prevented clogging of the fibrous mat pores and facilitated optical imaging of cells. Importantly, coatings on ES mats still retained pH responsive behavior as shown for PCPP + Poly B coatings (**SI Fig. S14B**). **Fig. 7B** summarizes Petrifilm^{TM} assay results for 6 BL PPz + Poly B coated ES mats challenged with 10^5 or 10^7 CFU/cm^2 *E. coli*. In this case, all coated ES mats could prevent the growth of even an extreme challenge of 10^7 CFU/cm^2. To further explore the full potential of the coatings, ES mats were repeatedly challenged with 10^5 CFU/cm^2 *E. coli* (**Fig. 7C**). Remarkably, regardless of the fluorination degree of PPz, all the coated ES mats were able to withstand triple bacterial attack. This result illustrates the high level of antibacterial activity, robustness, and durability of the coatings on ES mats.

Fig. 7E&F illustrates that, similarly to coatings on flat substrates, fluorination of PPzs included in the coatings on ES mats decreased cell coverage for FP77 and FP60 compared to PCPP coatings. Increased surface roughness seen in **Fig. 7A**, along with increased hydrophobicity for highly fluorinated coatings likely explains the differences observed in cell coverage. Further studies comparing cellular proliferation rates could be done in the future to confirm. Regardless of fluorination degree, a clear increase in live cell coverage is observed for all coatings on ES mats (**Fig. 7E&F**). Importantly, few, if any, dead (red) cells were observed on PPz + Abx coatings on ES mats (controls confirming staining efficacy **SI Fig. S15**).

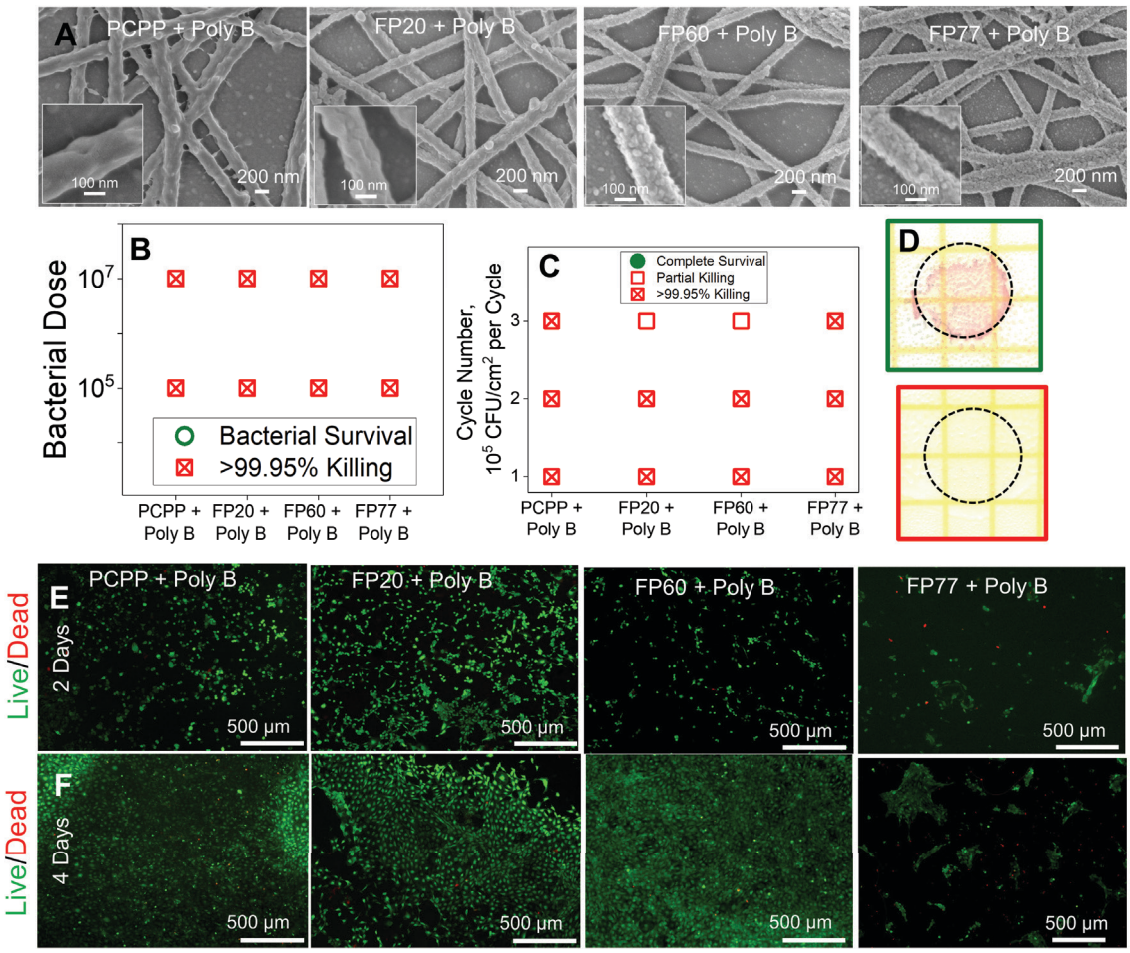

Fig. 7. (A) SEM images of 6 BL coatings of PPz + Poly B on PCL/Collagen ES mats. Petrifilm™ results of 6 BL PPz + Poly B coatings against 10^5 or 10^7 CFU/cm^2 *E. coli* (B) or repeated attacks of 10^5 CFU/cm^2 (C). (D) Representative images of samples completely covered and completely preventing bacterial growth. Live/dead staining of fibroblasts grown on 6 BL coatings of PPzs + Poly B for 2 (E) or 4 (F) days.

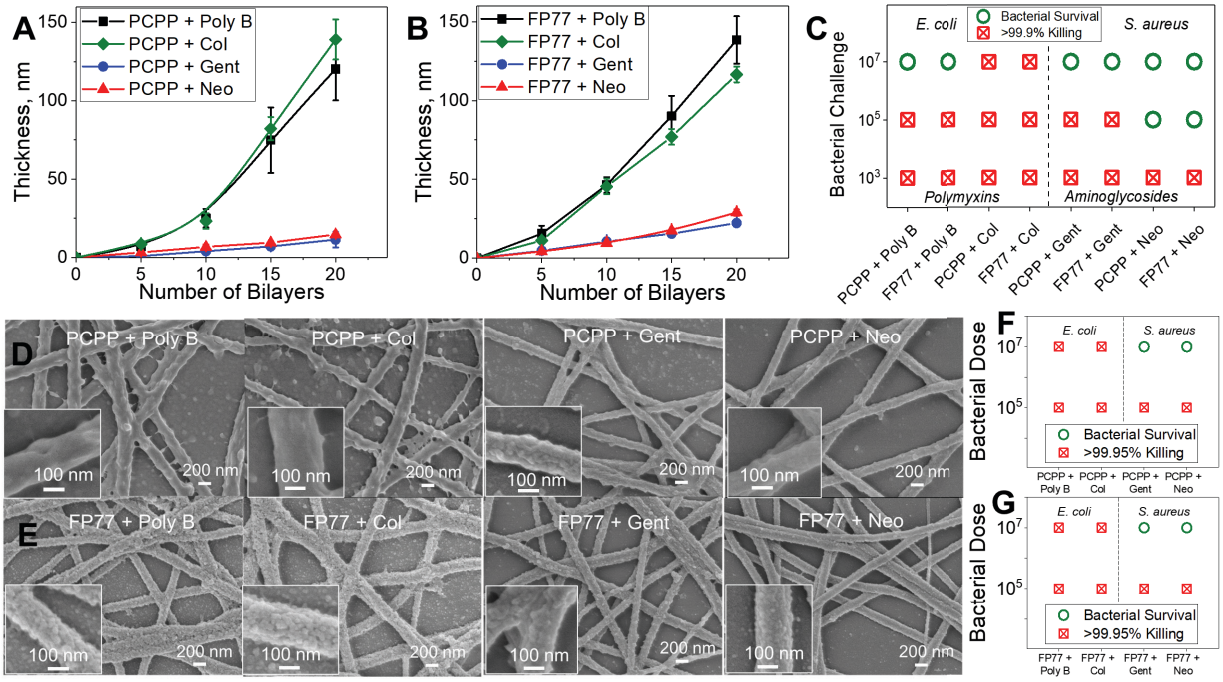

Fig. 8. LbL growth of PCPP (A) and FP77 (B) with a variety of cationic antimicrobial agents. (C) Petrifilm™ assay results demonstrating the efficacy of 10-nm PPz coatings with a variety of antibiotics against Gram-negative and Gram-positive bacteria. Assay run with 10^3, 10^5 or 10^7 (E) CFU on 1x1 cm^2 Si wafers. SEM images of 6 BL coatings of PCPP (D) or FP77 (E) with different antibiotics deposited on PCL/Collagen ES mats. Petrifilm results of 6 BL PCPP + Abx (F) and FP77 + Abx (G) coatings deposited on the ES mats against 10^5 or 10^7 CFU/cm^2 *E. coli* (for Poly B and Col coatings) or *S. aureus* (for Gent and Neo coatings).

While the results with Poly B are very promising, especially considering the low level of leachability, Poly B is typically considered a last resort antibiotic and may not be suitable for some patients. Therefore, we explored the potential of the PPz + antibiotic system with other cationic antibiotics, specifically colistin (Col), neomycin (Neo), and gentamicin (Gent). Colistin, also known as polymyxin E, is the only other polymyxin that is used clinically and may be beneficial for treating drug-resistant strains of bacteria.[56] Polymyxins are bactericidal, with their primary mechanism of action being disruption of bacterial membranes although other mechanisms of action are possible.[57] Alternatively, Gent and Neo are aminoglycosides, which are active by binding to the 30S ribosomal subunit.[58] Among PPzs with different fluorination degrees, we chose to focus on non-fluorinated PCPP and highly fluorinated FP77. **Fig. 8A &B** illustrates construction

of LbL coatings of these polymers with a range of antibiotics on Si wafers. Both PCPP and FP77 supported coating growth with all cationic antibiotics mentioned. However, uncharged antibiotics or those with only 1+ charge, just as clindamycin, were unable to support film growth. Similar to Poly B, Col is a polypeptide with a cyclic ring and hydrophobic tail, as such PPz + Col form coatings with similar thickness to PPz + Poly B coatings. In contrast, Neo and Gent are much smaller molecules, with only 3-4 positive charges at neutral pH (in contrast to 5 charges on Poly B). As such, PPz + Neo or Gent coatings are much thinner; for example, 20 bilayers of PCPP + Gent or Neo is ~20 nm while PCPP + Poly B or Col is ~ 125 nm. These results suggest that antibiotic hydrophobicity and charge number can be used as additional parameters to tune coating thickness, and that both antibiotic charge and hydrophobicity enhance coating deposition. Notably, comparing the pH-triggered drug release profiles from the more hydrophobic Poly B to the more hydrophilic Gent, no significant differences were observed suggesting that antibiotic hydrophobicity does not play a large role in controlling drug release.

Prior to antibacterial studies with PPz coatings involving Poly B, Col, Neo and Gent, we determined MICs of these antibiotics. These experiments, performed in solution against *E. coli* (ATCC 25922) and *S. aureus* (ATCC 12600) of various concentrations, yielded results shown in **SI Table S2**. All four antibiotics were active against gram-negative bacteria and had relatively low MICs (~2 μg/mL for Poly B or Col, <1 μg/mL for Gent, and 4-8 μg/mL for Neo against 10^5 CFU/mL of *E. coli*). However, Gent and Neo were also highly active against *S. aureus (*<1 μg/mL for Gent, and 4-8 μg/mL for Neo against 10^5 CFU/mL of *S. aureus)*. Therefore, Poly B- and Col-containing coatings were challenged with *E. coli*, and Gent- and Neo-containing coatings were tested against *S. aureus*. **Fig. 8C** shows the results of antibacterial studies on PCPP- and FP77-based antibiotic-containing coatings of 10-nm thickness deposited on Si wafers. Regardless of the polymer type, the coatings demonstrated antibacterial activity that corresponded to antibiotic MICs. For example, Neo has a higher MIC than Gent (4-8 *vs*. <1 μg/mL) and PPz + Gent coatings were able to prevent up to 10^5 CFU/cm^2 *S. aureus*, while PPz + Neo coatings were only able to prevent up to 10^3 CFU/cm^2 *S. aureus*. Therefore, both non-fluorinated and ionic fluorinated PPzs can be efficiently used to construct antibacterial coatings using several antibiotics, which carry positive charge.

Important for clinical translation, PPz coatings containing Col, Neo, or Gent could also be deposited on ES mats (**Fig. 8D**). As in the case of Poly B-containing coatings, deposition was stopped after 6 BL. As expected, Poly B and Col, which were shown to form thicker coatings on Si wafers (**Fig. 8A&B**) caused a bumpier morphology than Gent and Neo coatings. As proof-of-concept, 6 BL PCPP coatings of Poly B and Gent were deposited on an extra-thick batch of ES mat (to avoid LOD problems with LC-MS), dissolved, and solution concentrations of Poly B or Gent measured with LC-MS. A 6 BL PCPP + Poly B coating was found to contain ~27.2 µg or 2.3 $x10^{-8}$ mol/cm^2 of Poly B while a 6 BL PCPP + Gent coating was found to have ~11.5 µg or 2.4 $x10^{-8}$ mol/cm^2. Accounting for the different masses of both, PPz coatings show approximately the same molar loading per film mass/volume regardless of antibiotic hydrophobicity. Importantly, pH-triggered release of both antibiotics from PCPP coatings on ES mats was found to be indistinguishable (**SI Fig. S14B)**.

Fig. 8F&G shows the antibacterial activity of PCPP and FP77 coatings on ES mats against *E.coli* (for Poly B and Col coatings) and *S. aureus* (for Gent and Neo coatings). All coatings were able to prevent a challenge of 10^5 CFU/cm^2, while Poly B-based and Col-based coatings, which are known to be much thicker than Gent- and Neo- based coatings, were additionally able to completely prevent a challenge of 10^7 CFU/cm^2. As ES mats have a high surface area, these coatings are not surprisingly more active than coatings on flat substrates. These results show that just a few bilayers of thin coating can prevent extremely high bacterial challenge numbers from surviving. **SI Fig. S15** also shows the live/dead staining results of fibroblasts cultured for 2 days on PPz (PCPP or FP77) + Abx (Poly B, Col, Gent, or Neo)-coated ES mats, suggesting that the coated ES mats were not toxic to NIH/3T3 fibroblasts. With the most cyto-adhesive PPz - PCPP - 6 BL Poly B or Gent coatings were deposited on ES mats and used for a brief study with keratinocytes. Keratinocytes were cultured on samples for 2 days and then stained with either live/dead stains (**SI Fig. S16A**) or DAPI/phalloidin stains (**SI Fig. S16B**). Cell coverage on both coatings was comparable to a control bare ES mat. This result highlights that such coatings have promise in tissue engineering applications.

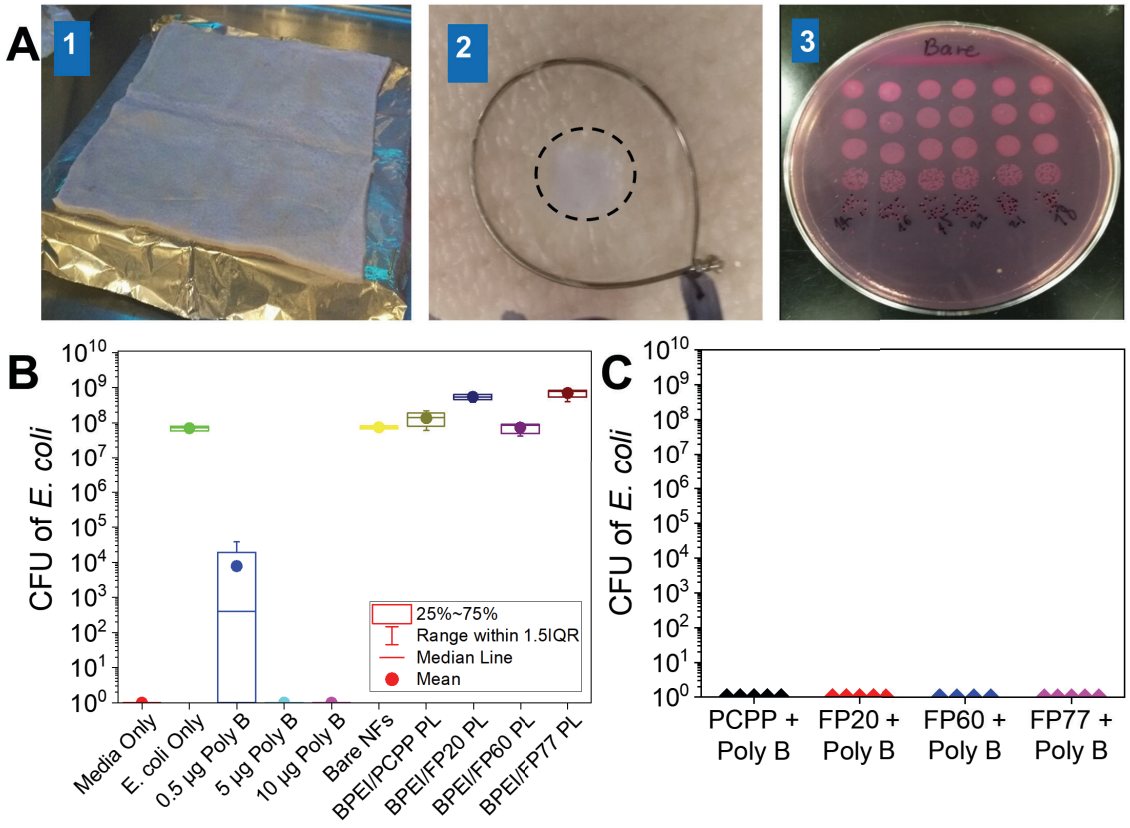

Fig. 9. Representative images of pig skin (A1), pig skin wounded, inoculated, and covered with an ES mat (A2) and spot plating of *E. coli* growth on MacConkey agar from pig skin post homogenization (A3). Quantification of *E. coli* growth on MacConkey agar from pig skin *via* spot plating post homogenization for control samples (B) and test samples (C). PPz + Poly B films were 6 BLs on ES mats, run in 5 replicates. Note: one ES mat suffered mechanical failure (detachment from ring) for FP60 coated samples, so that data point was removed. All 0 points displayed as one so that they are visible on a log scale. p-value < $1x10^{-4}$ for all treatments versus bare nanofibers.

Since *in vitro* studies of these coatings were promising, *ex vivo* infected pig skin studies were conducted to better elucidate the potential of these coatings in complex biological environments. Pig skin is well established to be an excellent model for wound infection[59-61] and healing of human skin.[62-64] For this experiment, circular wounds of ~ 5 mm were created on the pig skin acquired from Animal Technologies (**Fig. 9A1**) with the biopsy punch and scalpel, inoculated with 5×10^{4} CFU *E. coli*, and allowed to grow for 1 h at 37 ˚C before controls or ES

mats coated with 6 BL PPz + Poly B coatings of various fluorination degrees were applied (**Fig. 9A2**). Wounds had approximately ~ 7.7 ± 2.9 × 10^5 CFU of *E. coli* prior to the application of samples. The treated wounds were then incubated at 37 ˚C for 16 h, 5 mm biopsies were cut out of the skin, and homogenized. The homogenate was plated and counted after 18 h of incubation (**Fig. 9A3**). The results from this experiment can be seen for controls in **Fig. 9B** and for test samples in **Fig. 9C.** As controls, solutions of media only, *E. coli* only, or Poly B solutions (50, 1000 or 5000 μg/mL) were applied in 10 μL doses. The media only samples show that without the addition of *E. coli*, the native skin had no bacteria that show up on the MacConkey plates. The Poly B solutions showed that ~5 μg of Poly B applied to the surface was sufficient to drastically decrease the proliferation of *E. coli* on the skin. Controls of bare ES mats and prime layer coatings of PPzs on ES mats (Fig. 9B) did not decrease the bacterial load on the skin, indicating that all four PPzs as well as bare ES mats alone had no antibacterial effects. Importantly, all four 6 BL PPz + Poly B coatings were able to almost completely inhibited *E. coli* growth on the wounded pig skin (**Fig. 9C**), suggesting that these coatings can function even in complex biological environments.

Conclusions and Outlook:

In conclusion, we have demonstrated the direct, all aqueous deposition of a variety of cationic antibiotics with a family of fluorinated polyphosphazenes on a wide range of substrates from flat Si wafers and Ti plates to three-dimensional electrospun fiber matrices. All-aqueous deposition is an advantage for this system as traditional coatings require organic solvents. Fluorination degree of PPz used in assembly pre-determines antibiotic payload in films and can be efficiently used to build films that give a set dose of antibiotics in response to bacterial approach or pH trigger. Importantly, coatings of every PPz fluorination degree tested were able to prevent the growth of a high dosage of bacteria directly applied to the surface, even after 30 days of pre-exposure to bacteria-free physiological conditions, highlighting the durability and longevity of these films in terms of antibacterial activity. Moreover, when applied to substrates with high surface areas, extremely high antibiotic loads can be achieved with the deposition of just a few layers of coating. Additionally, such coatings on ES mats were able to defeat multiple attacks from bacteria. With careful antibiotic selection, the potency of the coatings towards gram-positive or gram-negative strains of bacteria can be easily tuned. In addition, to prevent drug-resistant bacteria from developing, the antimicrobial component can be switched to a cationic, antibacterial hybrid

that have been shown to be unlikely to induce antibiotic resistance. For example, other groups have developed antibiotic hybrids that have shown promise to not cause antibacterial resistance.[65,66]

Finally, one potential application of this material is as a wound dressing, and as such, these coatings would be exposed to a variety of environments and need to be on a flexible substrate. PPz coatings can efficiently deposit on electrospun materials and used as antibacterial coatings. In this case, the dressing would be changed periodically, thus unlikely to provide enough time for drug-resistant bacteria to develop. At the same time, these coatings display excellent hemolytic compatibility for two different blood types (rabbit and porcine) and cytocompatibility for fibroblasts and keratinocytes. Moreover, these novel coatings remain highly efficient even in an infected wound on pig skin. Taken together, this work demonstrates a versatile and highly adaptable antibiotic-containing coating system that can be applied to a wide range of biomedical applications.

Materials & Methods

Materials:

Tryptic soy broth (TSB) powder was obtained from MP biomedicals (Solon, OH). Difco™ Technical Agar was obtained from BD Biosciences (San Jose, CA). Polymyxin B, branched polyethylenimine (BPEI, weight-average molecular weight M_w of 750,000 g/mol), polycaprolactone (PCL, number-average molecular weight M_n of 80,000 g/mol), Titanium sheet, and sodium phosphate monobasic dihydrate were purchased from Sigma-Aldrich (Allentown, PA). Type I collagen was purchased from Elastin Products Company, Inc. (Owensville, MO). 1,1,1,3,3,3-hexafluoro-2-propanol (HFIP) was purchased from Oakwood Products, Inc. (Estill, SC). Hydrochloric acid, sodium hydroxide, and sulfuric acid were obtained from Alfa Aesar (Tewksbury, MA). Ultrapure water from a Milli-Q system (Merck Millipore, Burlington, MA, USA) with a resistivity of 18.2 MΩ was used in all experiments. Boron-doped silicon (Si) wafers were purchased from University Wafer, Inc. Glass coverslips for electrospun fiber preparation was bought from Carolina Biological Supply Company (Burlington, NC). All other chemicals were purchased from Sigma-Aldrich and used without further modification. This work uses several ionic, fluorinated polyphosphazenes, which were synthesized as described earlier.[23,25,28,67,68] M_ws were 800 kDa for PCPP, 140 kDa for FP20, 246 kDa for FP60, and 200 kDa for FP77.

Methods:

Electrospun Fibers Preparation: Glass coverslips (18-mm ⌀) were cleaned with isopropanol then coated with poly-l-lysine and blotted dry to improve the integrity and adherence of electrospun fibers. PCL/Collagen fibers were electrospun onto the prepared glass coverslips as previously described.[69] Briefly, a 4% w/v solution of 3:1 PCL:type I collagen in HFIP was loaded into a syringe fitted with a blunted 21G needle and electrospun onto the glass substrates (which were laid on top of grounded aluminum foil) at a flow rate of 10 μL/min through an electric field of 12 kV/12 cm. Ambient conditions during electrospinning were 45% relative humidity and 23 °C.

Layer-by-Layer Deposition: Films of PPzs and Poly B were deposited using the dip-deposition technique. In order to deposit PPzs + Poly B films onto surfaces, first a priming layer of BPEI (M_W = 750 kDa, pH 9, 0.2 mg/mL) was deposited for 15 min followed by a priming layer of PPz (pH 7.5, 0.01 M phosphate buffer (PB), 0.4 mg/mL) deposited for 10 minutes. Afterwards, alternating layers of Poly B (pH 7.5, 0.5 mg/mL) and PPzs (pH 7.5, 0.4 mg/mL) were deposited for 10 min.

Dry and Wet Thickness Measurements: Thicknesses and optical constants in dry states were characterized by a variable angle spectroscopic ellipsometer (VASE, M-2000 UV−visible−NIR (240−1700 nm) J. A. Woollam Co., Inc., Lincoln, NE, USA) equipped with a temperature-controlled liquid cell. Dry measurements were carried out at four angles of incidence: 45°, 55°, 65°, and 75°. For data fitting, polymeric layers were treated as a Cauchy material of thickness d with refractive index A. Both parameters were fit simultaneously. *In situ* ellipsometry was conducted at an angle of 75° with a liquid cell and temperature controller. Samples (~30 to 50 nm) were run in PBS at pH 7.5 at 37 °C for 1 h. To calculate swelling ratio, the wet thickness for the last ten minutes (*i.e.* minutes 50 to 60) were used in order to provide enough time to make sure the film was at equilibrium. More details for fitting models can be found in an earlier publication.[25]

Degradation/stability at 37 °C studies: 100-nm coatings on 1x1 cm^2 Si wafers were first washed with PBS at pH 7.5, dried, and thickness measured to separate the effect of salt on the coatings from the effects of pH and temperature. Afterwards, samples were exposed to 10 mL of PBS at

pH 7.5 or 5.5. After the desired soak time, samples were washed with pH matched 0.01 M PB, dried with nitrogen, and returned to the same solution. Samples were run in duplicate.

Liquid Chromatography-Mass Spectrometry (LC-MS): For LC-MS analysis, 1x1 cm^2 samples were exposed to 0.5 mL of PBS at pH 7.5, 6.5, 5.5, 4.5, and 12 consecutively, for 1 h each and solutions used for LC-MS analysis at the Integrated Metabolomics Analysis Core. After exposure to a certain pH, samples were rinsed with phosphate buffer at matched pH, dried, and thickness measured with ellipsometry. Duplicate sample sets were used to ensure reproducibility. The target compounds from the collected PBS samples were detected and quantified on a triple quadrupole mass spectrometer (Altis, Thermo Scientific, Waltham, MA) coupled to a binary pump HPLC (Vanquish, Thermo Scientific). Since Poly B is a mixture of five different structures with slightly different R groups, with Poly B1 and B2 being the major components, the 2+ and 3+ ions of Poly B1 and Poly B2 were tracked for analysis. The specific *m/z* of the product and parent ions monitored are listed in **Table 1**. MS parameters were optimized for the target compound under direct infusion at 5 µL/min to identify the SRM transitions (precursor/product fragment ion pair) with the highest intensity (**Table 1**) Samples were maintained at 4 °C on an autosampler before injection. The injection volume was 10 µL. Chromatographic separation was achieved on a Hypersil Gold 5 µm 50 x 3 mm column (Thermo Scientific) maintained at 30 °C using a solvent gradient method. Solvent A was water (0.1% formic acid). Solvent B was acetonitrile (0.1% formic acid). The gradient method used was 0-1 min (20% B to 60% B), 1-1.5 min (60% B to 95% B), 1.5-3 min (95% B), 3-4.1 min (95% B to 20% B), 4.1-5 min (20% B). The flow rate was 0.5 mL/min. Sample acquisition and analysis was performed with TraceFinder 4.1 (Thermo Scientific). Measured concentrations of Poly B as well as release volumes were used to calculate antibiotic content in the films and then normalized by film thickness

Table 1: Quantitative SRM Transitions for compounds

Compound	**Polarity**	**Precursor (m/z)**	**Product (m/z)**	**Collision Energy (V)**	**RF Lens (V)**
Polymyxin B1 2+	Negative	603.0	593.6	16.52	162
Polymyxin B1 3+	Negative	403.0	396.7	10.23	79
Polymyxin B2 2+	Negative	596.8	587.4	16.26	174
Polymyxin B2 3+	Negative	398.0	391.8	10.23	84

Solution Interactions Studies: Dynamic light scattering studies were conducted using Malvern Zetasizer Nano series instrument (Malvern Instruments Ltd., Worcestershire, UK). The experiments were carried out in 50 mM phosphate buffer, pH 7.4 (PB) with 0.5 mg/mL initial polymer concentration.

Fiber Diameter Calculations: To determine the diameter of fibers in ES mats, 20 measurements were made per image using ImageJ for two images for each sample.

Bacterial Studies: Bacterial strains in this work include *Escherichia coli* (*E. coli*) ATCC 25922 and *Staphylococcus aureus* (*S. aureus*) ATCC 12600. *E. coli* and *S. aureus* were streaked on TSB agar plates from a frozen glycerol stock, incubated at 37 °C for 16 h to obtain single colonies, and stored at 4 °C before bacterial culture. All cultures were started with colonies from plates of less than one week old.

Minimum Inhibitory Concentration (MIC) Assays: The MICs of Poly B, Col, Gent, and Neo for *E. coli* and *S. aureus* were determined by the standard method of measuring optical density at 600 nm (OD_{600}). Specifically, a single colony was isolated and grown overnight in TSB for 16 h at 37 °C, 250 rpm. Afterwards, OD_{600} was measured and used to calculate the CFU/mL and the culture was diluted to the desired concentration (2 x, 10^3, 10^5 or 10^7 CFU/mL) in TSB. 100 µL of bacterial culture was added to 100 µL of antibiotic in various concentrations and cultured for 24 h in 37 °C (static). OD_{600} of the culture was measured after 24 h using a 96 well plate reader. Each antibiotic concentration was tested in triplicate against each bacterial concentration. Three dilutions of each bacterial culture used were plated to verify the count (CFU/mL) used in the test. TSB and bacteria only tubes were used as controls.

Bacterial Growth Curves: A single colony of *E. coli* was isolated and grown overnight in 3 mL of TSB for 16 h at 37 °C, 250 rpm. The OD_{600} was measured and used to calculate the CFU/mL and the culture was diluted to 10^5 CFU/mL in TSB. 12 mL of 10^5 CFU/mL in TSB was placed in a 6 well plate with either nothing (control), various concentrations of Poly B, or PPz/Poly B samples on 1x1 cm^2 Si wafers. A volume of 12 mL was chosen so that a maximum concentration

less than MIC could be achieved assuming the worst case scenario in which all Poly B was released from the most potent coating PCPP/Poly B 200 nm, which contains ~20 μg of Poly B. OD_{600} was measured every 2 hours starting at hour 4 until 14 h. All samples were run in triplicate. Data show represent averages of three data sets with error bars representing the standard.

Petrifilm Assays: For Petrifilm assays, a single colony was inoculated in 3 mL of TSB and grown overnight at 37 °C, 250 rpm. Afterwards, the OD_{600} of the culture was measured and used as a guideline to prepare cultures containing 10^9 and 10^7 CFU/mL *via* dilution with TSB. 3M™ Petrifilm™ *E. coli* count plates were treated with 1 mL of sterilized DI water for 30 min to hydrate the nutrient loaded gel layer. PPz + Poly B coated silicon wafers were placed face up on the hydrated Petrifilms and 5 μL of bacterial suspension was placed onto the sample and incubated at 37 °C for 24 h. After 24 h, the bacterial colonies appearing on top of the samples were counted while bacteria off the edges of the sample were not counted. All samples were tested in duplicate.

Zone of Inhibition Assay: A single colony was isolated and grown overnight in 3 mL of TSB for 16 h at 37 °C, 250 rpm. Afterwards, OD_{600} was measured and used to calculate the CFU/mL and the culture was diluted to 10^5 CFU/mL. *E. coli* was streaked onto 20 mL TSB agar plates from the stock solution, three times with 60-degree rotation each time. A 1x1 cm^2 sample on Si wafer was placed face down on the agar and the plate incubated for 24 h at 37 °C. Samples were run in duplicate with PCPP and FP77 + Poly B coatings of 100 nm thickness.

Cell Studies:

Studies on Flat Substrates: NIH/3T3 fibroblasts were purchased from the American Type Culture Collection (ATCC, USA). Cells were cultured in Dulbecco's modified Eagle's medium (HyClone) supplemented with 10% fetal bovine serum (v/v) (Atlanta Biologicals), 1% Non-Essential Aminoacids (HyClone), 10 μM HEPES (HyClone) and 1% penicillin/streptomycin (Corning). Cells were propagated following ATCC standard protocols. Prior to cell studies, PPz + Poly B coating samples on Si wafers were sterilized with UV light inside a biosafety cabinet for 10 minutes per side. For culturing, samples were placed inside a 24-well plate, covered with a cell suspension at a seeding density of 10^4 cells/cm^2 in 1 mL of fresh media, and incubated at 37 °C in a 10% CO_2 atmosphere for 2 or 4 days. For Live/Dead staining, the media was removed, samples

were washed with 250 μL of 1X Phosphate-Buffered Saline (PBS) at room temperature, and they were overlaid with a staining solution of 2 μM Calcein AM (Enzo Life Sciences) and 3 μM Propidium Iodine (Enzo Life Sciences) in PBS. A positive control (cells grown without exposure to sample) and negative control (cells fixed with 70% ethanol in water for 30 minutes at 4 °C before staining) were included. After 30 minutes of incubation at room temperature while protected from light, each sample was imaged using confocal microscopy (Leica DMi8) at five independent regions in the surface. Total cell count per region was calculated using ImageJ.

Studies on Electrospun Fiber Matrices as Substrates: NIH/3T3 fibroblasts were cultured in complete medium consisting of high glucose Dulbecco's Modified Eagle's Medium (Gibco Cat No. 12800) supplemented with 1.5 g/L sodium bicarbonate and 10% bovine calf serum (v/v). Samples (ES mats on 18-mm ⌀ glass coverslips) were placed inside a 12-well plate and sterilized by UV light inside a biosafety cabinet for 15 minutes per side. As needed, samples were then submerged in sterile phosphate-buffered saline (PBS) for up to an hour, in order to overcome the high hydrophobicity attributed by the ES mats, which would otherwise prevent homogeneous cell seeding. Cells were seeded onto the samples at 10,000 cells per cm^2 with 1 mL complete media, and the samples were incubated at 37 °C with 5% CO_2, 95% humidity for 2 or 4 days whereupon cell viability was determined by fluorescent staining with a Live/Dead kit (Invitrogen Cat No. L3224). One at a time, samples were removed and rinsed with warm PBS, submerged in 1 mL staining solution (PBS containing 2 μM calcein AM, 4 μM ethidium homodimer-1), and placed back in the 37 °C incubator for 5 minutes. The staining solution was then removed and the samples were rinsed with warm PBS, mounted on a microscope slide, and immediately imaged at 5 independent locations using a Nikon Eclipse 80i fluorescence microscope. A positive control (cells grown on bare ES mats) and negative control (cells grown on bare ES mats and fixed with 70% isopropanol in water for 30 minutes at RT prior to staining) were included.

Hemolysis Studies: Hemocompatibility tests were conducted using a modified hemolysis test with red blood cells, RBCs (1% suspension in PBS, 2 h incubation at 37 °C)[42-45] and using whole rabbit blood (1.0 mL, 2 mg/mL hemoglobin, 4 h incubation at 37 °C).[25,41]

Human Cell Studies:

Human keratinocytes immortalized by expressing the catalytic subunit of telomerase were a gift from Dr. James Rheinwald (NIH Harvard Skin Disease Research Center). Cells were plated in serum-free keratinocyte medium supplemented with recombinant epidermal growth factor (2.5 mg/500 mL), bovine pituitary extract (25 mg/500 mL) (Invitrogen, Carlsbad, CA), 0.3 mM $CaCl_2$ (Sigma), 100 mg/mL streptomycin, and 100 IU/mL of penicillin (Sigma, St Louis, MO) and cultured at 37 °C in a humidified 5% CO_2 atmosphere. The medium was replaced every 48 h until they reached 60-70% confluence. Keratinocytes were seeded onto various ES mats at a density of 5×10^3 cells/cm^2 and allowed to attach for 20 min prior to addition of fully supplemented medium. The cells were further cultured for up to 2 days.

Live/Dead Staining: Invitrogen™ LIVE/DEAD™ Viability/Cytotoxicity Kit for mammalian cells was used. It contains Calcein AM (Component A, 40 µL 4 mM in anhydrous DMSO) and Ethidium homodimer-1 (Component B, 200 µL 2 mM in DMSO/H2O 1:4 (v/v)). 1 µL Component A and 4 µL Component B solutions were mixed and diluted into 2 mL DPBS. For each 6-well sample, 2 mL A/B mixture solutions were required. Samples were rinsed with DPBS first and then cultured in A/B mixture solution for 20 min. After incubation, the samples were washed with DPBS and then imaged with a Nikon Eclipse 80i epifluorescent microscope.

Immunofluorescent microscopy: Immunofluorescent staining of cells was performed following the procedures previously described.[70] Briefly, cultured cells were fixed in 4% paraformaldehyde (Sigma) for 10 min and then permeabilized with 0.3% Triton X-100 (Sigma) in PBS for 5 min, and followed by 3% BSA (Sigma) in PBS for 30 min. The samples were rinsed with PBS for 3 times prior to incubation with phalloidin-TRITC (Sigma, 1:150) for 30 min. Cell nuclei were stained with DAPI (Sigma, 1:1000). The stained samples were examined under a Nikon Eclipse 80i epifluorescent microscope.

Ex-vivo Porcine Skin Studies:

Fresh, shaved porcine skin without subcutaneous tissue was purchased from Animal Technologies, Inc. and used within 18 h of harvesting. Both sides of the skin were treated with UV light in a biosafety cabinet for 15 min before use in order to reduce its intrinsic bacterial load. Using aseptic

techniques, the skin was trimmed into 1”x1” sections, and a 5-mm diameter wound was created by removing the stratum corneum using a biopsy punch and a scalpel.

E. coli ATCC 25922 was grown overnight in 10 mL of TSB for 16 h at 37 °C, 250 rpm. For wound inoculation, 10 µL of a cell suspension containing 5×10^4 CFU of *E. coli* in TSB was applied onto the exposed epidermis and incubated for 1 h at 37 °C. Then, the wounds were treated with either 10 µL of sterile saline (0.9% NaCl in water), 10 uL of a solution containing 10, 5 or 0.5 µg of Polymyxin B in saline, or ES mats deposited with 6 bilayers of either PPzs + Poly B or prime layer control (BPEI + PPz). In order to ensure continuous contact between the mats and the surface of the wound, 50 µL of saline were added on the mats to keep the surfaces wet and stuck together during incubation. The samples were incubated for 16 h at 37 °C with five replicates per condition.

After incubation, each mat was removed from the wound and rinsed with 1 mL of saline in order to collect the bacterial cells that remained attached to it. Then, each wound was excised using a 5 mm biopsy punch. This biopsy was added to the collected saline from the previous step and homogenized at 35,000 rpm for 1 min using a tissue homogenizer (Omni International). Sample homogenates were serially diluted in saline, and 2.5 µL of each dilution were spot-plated on MacConkey agar plates (Becton Dickinson) and incubated at 37 °C for 18 h. For estimating the bacterial load of the samples, only lactose-positive colonies surrounded by precipitated bile salts corresponding to *E. coli* were counted (no such colonies were identified as part of the intrinsic bacterial load of the pig skin).

Author Information:

Corresponding author: Svetlana Sukhishvili, svetlana@tamu.edu

Authors declare no competing interests.

Author Contributions:

V.A., S. S., and A.A. designed the study and wrote the manuscript. V.A. and J.Z. prepared samples for all studies and measured physiochemical characteristics of films. V.A. performed bacterial studies. D.P. performed cell studies on flat substrates and *ex vivo* pig skin studies. A.M. synthesized polymers, performed DLS, hemolysis and protein adsorption studies. M.S. electrospun

fiber matrices, and performed cell studies on ES mats. H.H. took SEM images and provided help with manuscript preparation. A. J. and H. W. reviewed and edited the manuscript.

Acknowledgements:

This work was supported by the National Science Foundation under Award DMR-1808483 (S.S.) and DMR-1808531 (A.A.) and partially by NIAMS award number 1R01AR067859 (H.W.). V.A. acknowledges financial support from Texas A&M University/Association of Former Students Graduate Merit Fellowship and Texas A&M Engineering Experiment Station (TEES). M.S. was supported by the Robert Crooks Stanley Graduate Fellowship in Engineering and Science. Authors are grateful to Samantha Hernandez, Danielle Yarbrough, and Christian Frey, who participated in this work through the Aggie Research Program, for help with sample preparation and Dr. Papatya Kaner (University of Maryland) for assistance with conducting DLS experiments. Authors are grateful to Yuhao Wang (Former SIT) for conducting experiments with keratinocytes. Authors acknowledge use of the Integrated Metabolomics Analysis Core and the Materials Characterization Facility at Texas A&M University. Authors thank Jordan Brito for preparing final samples for the ex vivo pig skin study.

References:

(1) Vasilev, K.; Cook, J.; Griesser, H. J. Antibacterial surfaces for biomedical devices. *Expert Review of Medical Devices* **2009**, *6*, 553-567.

(2) Busscher, H. J.; van der Mei, H. C.; Subbiahdoss, G.; Jutte, P. C.; van den Dungen, J. J. A. M.; Zaat, S. A. J.; Schultz, M. J.; Grainger, D. W. Biomaterial-Associated Infection: Locating the Finish Line in the Race for the Surface. *Science Translational Medicine* **2012**, *4*, 153rv110.

(3) Coad, B. R.; Griesser, H. J.; Peleg, A. Y.; Traven, A. Anti-infective Surface Coatings: Design and Therapeutic Promise against Device-Associated Infections. *PLOS Pathogens* **2016**, *12*, e1005598.

(4) Ventola, C. L. The antibiotic resistance crisis: part 1: causes and threats. *P T* **2015**, *40*, 277-283.

(5) Zhuk, I.; Jariwala, F.; Attygalle, A. B.; Wu, Y.; Libera, M. R.; Sukhishvili, S. A. Self-Defensive Layer-by-Layer Films with Bacteria-Triggered Antibiotic Release. *ACS Nano* **2014**, *8*, 7733-7745.

(6) Albright, V.; Zhuk, I.; Wang, Y.; Selin, V.; van de Belt-Gritter, B.; Busscher, H. J.; van der Mei, H. C.; Sukhishvili, S. A. Self-defensive antibiotic-loaded layer-by-layer coatings: Imaging of localized bacterial acidification and pH-triggering of antibiotic release. *Acta Biomaterialia* **2017**, *61*, 66-74.

(7) Pavlukhina, S.; Zhuk, I.; Mentbayeva, A.; Rautenberg, E.; Chang, W.; Yu, X.; van de Belt-Gritter, B.; Busscher, H. J.; van der Mei, H. C.; Sukhishvili, S. A. Small-molecule-hosting nanocomposite films with multiple bacteria-triggered responses. *NPG Asia Mater* **2014**, *6*, e121.

(8) Komnatnyy, V. V.; Chiang, W.-C.; Tolker-Nielsen, T.; Givskov, M.; Nielsen, T. E. Bacteria-Triggered Release of Antimicrobial Agents. *Angewandte Chemie International Edition* **2014**, *53*, 439-441.

(9) Cado, G.; Aslam, R.; Séon, L.; Garnier, T.; Fabre, R.; Parat, A.; Chassepot, A.; Voegel, J. C.; Senger, B.; Schneider, F.; Frère, Y.; Jierry, L.; Schaaf, P.; Kerdjoudj, H.; Metz-Boutigue, M. H.; Boulmedais, F. Self-Defensive Biomaterial Coating Against Bacteria and Yeasts: Polysaccharide Multilayer Film with Embedded Antimicrobial Peptide. *Advanced Functional Materials* **2013**, *23*, 4801-4809.

(10) Liang, J.; Wang, H.; Libera, M. Biomaterial surfaces self-defensive against bacteria by contact transfer of antimicrobials. *Biomaterials* **2019**, *204*, 25-35.

(11) Decher, G.; Hong, J.-D. Buildup of ultrathin multilayer films by a self-assembly process, 1 consecutive adsorption of anionic and cationic bipolar amphiphiles on charged surfaces. *Makromolekulare Chemie. Macromolecular Symposia* **1991**, *46*, 321-327.

(12) Hizal, F.; Zhuk, I.; Sukhishvili, S.; Busscher, H. J.; van der Mei, H. C.; Choi, C.-H. Impact of 3D Hierarchical Nanostructures on the Antibacterial Efficacy of a Bacteria-Triggered Self-Defensive Antibiotic Coating. *ACS Applied Materials & Interfaces* **2015**, *7*, 20304-20313.

(13) Suleimenov, I.; Güven, O.; Mun, G.; Beissegul, A.; Panchenko, S.; Ivlev, R. The formation of interpolymer complexes and hydrophilic associates of poly(acrylic acid) and non-ionic copolymers based on 2-hydroxyethylacrylate in aqueous solutions. *Polymer International* **2013**, *62*, 1310-1315.

(14) Chuang, H. F.; Smith, R. C.; Hammond, P. T. Polyelectrolyte Multilayers for Tunable Release of Antibiotics. *Biomacromolecules* **2008**, *9*, 1660-1668.

(15) Moskowitz, J. S.; Blaisse, M. R.; Samuel, R. E.; Hsu, H.-P.; Harris, M. B.; Martin, S. D.; Lee, J. C.; Spector, M.; Hammond, P. T. The effectiveness of the controlled release of gentamicin from polyelectrolyte multilayers in the treatment of Staphylococcus aureus infection in a rabbit bone model. *Biomaterials* **2010**, *31*, 6019-6030.

(16) Hung, C.-R.; Lee, C.-H. Protective Effect of Cimetidine on Tannic Acid-induced Gastric Damage in Rats. *Journal of Pharmacy and Pharmacology* **1991**, *43*, 559-563.

(17) Field, J. A.; Lettinga, G.: Toxicity of Tannic Compounds to Microorganisms. In *Plant Polyphenols: Synthesis, Properties, Significance*; Hemingway, R. W., Laks, P. E., Eds.; Springer US: Boston, MA, 1992; pp 673-692.

(18) *Polyphosphazenes for Biomedical Applications*; Andrianov, A. K., Ed.; John Wiley & Sons: Hoboken, New Jersey, 2009, pp 457.

(19) *Polyphosphazenes in Biomedicine, Engineering & Pioneering Synthesis*; Andrianov, A. K.; Allcock, H. R., Eds.; American Chemical Society: Washington, DC, 2018; Vol. 1298, ACS Symposium Series.

(20) Bates, M. C.; Yousaf, A.; Sun, L.; Barakat, M.; Kueller, A. Translational Research and Early Favorable Clinical Results of a Novel Polyphosphazene (Polyzene-F) Nanocoating. *Regen. Eng. Transl. Med.* **2019**, 1-13.

(21) U.S. Food & Drug Administration 510(k) Premarket Notification. https://www.accessdata.fda.gov/scripts/cdrh/cfdocs/cfpmn/pmn.cfm?ID=K132675 (accessed 01.23.2018.

(22) U.S. Food & Drug Administration Premarket Approval (PMA). https://www.accessdata.fda.gov/scripts/cdrh/cfdocs/cfPMA/pma.cfm?id=P160014.

(23) Andrianov, A. K.; Svirkin, Y. Y.; LeGolvan, M. P. Synthesis and biologically relevant properties of polyphosphazene polyacids. *Biomacromolecules* **2004**, *5*, 1999-2006.

(24) Andrianov, A. K.; Marin, A.; Peterson, P.; Chen, J. Fluorinated polyphosphazene polyelectrolytes. *J. Appl. Polym. Sci.* **2007**, *103*, 53-58.

(25) Selin, V.; Albright, V.; Ankner, J. F.; Marin, A.; Andrianov, A. K.; Sukhishvili, S. A. Biocompatible Nanocoatings of Fluorinated Polyphosphazenes through Aqueous Assembly. *ACS Applied Materials & Interfaces* **2018**, *10*, 9756-9764.

(26) Allcock, H. R.; Kwon, S. An ionically crosslinkable polyphosphazene: poly[bis(carboxylatophenoxy)phosphazene] and its hydrogels and membranes. *Macromolecules* **1989**, *22*, 75-79.

(27) Cohen, S.; Bano, M. C.; Visscher, K. B.; Chow, M.; Allcock, H. R.; Langer, R. Ionically crosslinkable polyphosphazene: a novel polymer for microencapsulation. *Journal of the American Chemical Society* **1990**, *112*, 7832-7833.

(28) Andrianov, A. K.; Marin, A.; Peterson, P.; Chen, J. Fluorinated polyphosphazene polyelectrolytes. *J. Appl. Polym. Sci.* **2007**, *103*, 53-58.

(29) Andrianov, A. K.; Chen, J.; Payne, L. G. Preparation of hydrogel microspheres by coacervation of aqueous polyphosphazene solutions. *Biomaterials* **1998**, *19*, 109-115.

(30) Andrianov, A. K.; Marin, A.; Roberts, B. E. Polyphosphazene Polyelectrolytes: A Link between the Formation of Noncovalent Complexes with Antigenic Proteins and Immunostimulating Activity. *Biomacromolecules* **2005**, *6*, 1375-1379.

(31) Andrianov, A. K.; Marin, A.; Fuerst, T. R. Molecular-Level Interactions of Polyphosphazene Immunoadjuvants and Their Potential Role in Antigen Presentation and Cell Stimulation. *Biomacromolecules* **2016**, *17*, 3732-3742.

(32) DeCollibus, D. P.; Marin, A.; Andrianov, A. K. Effect of Environmental Factors on Hydrolytic Degradation of Water-Soluble Polyphosphazene Polyelectrolyte in Aqueous Solutions. *Biomacromolecules* **2010**, *11*, 2033-2038.

(33) Andrianov, A. K.; LeGolvan, M. P.; Sule, S. S.; Payne, L. G. Degradation of poly[di(carboxylatophenoxy)phosphazene] in aqueous solution. *PMSE Preprints* **1997**, *76*, 369-370.

(34) Ulusan, S.; Bütün, V.; Banerjee, S.; Erel-Goktepe, I. Biologically Functional Ultrathin Films Made of Zwitterionic Block Copolymer Micelles. *Langmuir* **2019**, *35*, 1156-1171.

(35) He, M.; Wang, Q.; Zhao, W.; Zhao, C. A substrate-independent ultrathin hydrogel film as an antifouling and antibacterial layer for a microfiltration membrane anchored via a layer-by-layer thiol–ene click reaction. *Journal of Materials Chemistry B* **2018**, *6*, 3904-3913.

(36) Smith, S. M. D-lactic acid production as a monitor of the effectiveness of antimicrobial agents. *Antimicrobial Agents and Chemotherapy* **1991**, *35*, 237-241.

(37) Andersen, K. B.; von Meyenburg, K. Are growth rates of Escherichia coli in batch cultures limited by respiration? *Journal of Bacteriology* **1980**, *144*, 114-123.

(38) Poirel, L.; Jayol, A.; Nordmann, P. Polymyxins: Antibacterial Activity, Susceptibility Testing, and Resistance Mechanisms Encoded by Plasmids or Chromosomes. *Clinical Microbiology Reviews* **2017**, *30*, 557.

(39) Allcock, H. R.; Pucher, S. R.; Fitzpatrick, R. J.; Rashid, K. Antibacterial activity and mutagenicity studies of water-soluble phosphazene high polymers. *Biomaterials* **1992**, *13*, 857-862.

(40) Liu, X.; Zhang, H.; Tian, Z.; Sen, A.; Allcock, H. R. Preparation of quaternized organic-inorganic hybrid brush polyphosphazene-co-poly[2-(dimethylamino)ethyl methacrylate] electrospun fibers and their antibacterial properties. *Polymer Chemistry* **2012**, *3*, 2082-2091.

(41) Henkelman, S.; Rakhorst, G.; Blanton, J.; van Oeveren, W. Standardization of incubation conditions for hemolysis testing of biomaterials. *Mater. Sci. Eng.: C Mater. Biol. Appl.* **2009**, *29*, 1650-1654.

(42) Yessine, M.-A.; Leroux, J.-C. Membrane-destabilizing polyanions: interaction with lipid bilayers and endosomal escape of biomacromolecules. *Advanced drug delivery reviews* **2004**, *56*, 999-1021.

(43) Lackey, C. A.; Murthy, N.; Press, O. W.; Tirrell, D. A.; Hoffman, A. S.; Stayton, P. S. Hemolytic activity of pH-responsive polymer-streptavidin bioconjugates. *Bioconjugate chemistry* **1999**, *10*, 401-405.

(44) Rozema, D. B.; Ekena, K.; Lewis, D. L.; Loomis, A. G.; Wolff, J. A. Endosomolysis by masking of a membrane-active agent (EMMA) for cytoplasmic release of macromolecules. *Bioconjugate chemistry* **2003**, *14*, 51-57.

(45) Andrianov, A. K.; Marin, A.; Fuerst, T. R. Self-assembly of polyphosphazene immunoadjuvant with poly(ethylene oxide) enables advanced nanoscale delivery modalities and regulated pH-dependent cellular membrane activity. *Heliyon* **2016**, *2*, Article e00102.

(46) Cutlip, D. E.; Garratt, K. N.; Novack, V.; Barakat, M.; Meraj, P.; Maillard, L.; Erglis, A.; Jauhar, R.; Popma, J. J.; Stoler, R.; Silber, S. 9-Month Clinical and Angiographic Outcomes of the COBRA Polyzene-F NanoCoated Coronary Stent System. *JACC: Cardiovascular Interventions* **2017**, *10*, 160-167.

(47) Styllou, P.; Silber, S. A case report of the new Polyzene™-F COBRA PzF™ Nanocoated Coronary Stent System (NCS): Addressing an unmet clinical need. *Cardiovascular Revascularization Medicine* **2016**, *17*, 209-211.

(48) Verret, V.; Wassef, M.; Pelage, J. P.; Ghegediban, S. H.; Jouneau, L.; Moine, L.; Labarre, D.; Golzarian, J.; Schwartz-Cornil, I.; Laurent, A. Influence of degradation on inflammatory profile of polyphosphazene coated PMMA and trisacryl gelatin microspheres in a sheep uterine artery embolization model. *Biomaterials* **2011**, *32*, 339-351.

(49) Thongcharoen, P.; Suriyanon, V.; Paris, R. M.; Khamboonruang, C.; de Souza, M. S.; Ratto-Kim, S.; Karnasuta, C.; Polonis, V. R.; Baglyos, L.; El Habib, R. A Phase 1/2 Comparative Vaccine Trial of the Safety and Immunogenicity of a CRF01_AE (Subtype E) Candidate Vaccine: ALVAC-HIV (vCP1521) Prime With Oligomeric gp160 (92TH023/LAI-DID) or Bivalent gp120 (CM235/SF2) Boost. *JAIDS Journal of Acquired Immune Deficiency Syndromes* **2007**, *46*, 48.

(50) Lu, Y.; Wu, Y.; Liang, J.; Libera, M. R.; Sukhishvili, S. A. Self-defensive antibacterial layer-by-layer hydrogel coatings with pH-triggered hydrophobicity. *Biomaterials* **2015**, *45*, 64-71.

(51) Morán, M. C.; Ruano, G.; Cirisano, F.; Ferrari, M. Mammalian cell viability on hydrophobic and superhydrophobic fabrics. *Materials Science and Engineering: C* **2019**, *99*, 241-247.

(52) Santos, G. The Importance of Metallic Materials as Biomaterials. *Adv Tissue Eng Regen Med Open Access* **2017**, *3*, 00054.

(53) Yang, X.; Ogbolu, K. R.; Wang, H. Multifunctional nanofibrous scaffold for tissue engineering. *Journal of Experimental Nanoscience* **2008**, *3*, 329-345.

(54) Albright, V.; Xu, M.; Palanisamy, A.; Cheng, J.; Stack, M.; Zhang, B.; Jayaraman, A.; Sukhishvili, S. A.; Wang, H. Micelle-Coated, Hierarchically Structured Nanofibers with Dual-Release Capability for Accelerated Wound Healing and Infection Control. *Adv Healthc Mater* **2018**, *7*, e1800132.

(55) Chen, J.; Zhan, Y.; Wang, Y.; Han, D.; Tao, B.; Luo, Z.; Ma, S.; Wang, Q.; Li, X.; Fan, L.; Li, C.; Deng, H.; Cao, F. Chitosan/silk fibroin modified nanofibrous patches with mesenchymal stem cells prevent heart remodeling post-myocardial infarction in rats. *Acta Biomaterialia* **2018**, *80*, 154-168.

(56) Landman, D.; Georgescu, C.; Martin, D. A.; Quale, J. Polymyxins Revisited. *Clinical microbiology reviews* **2008**, *21*, 449-465.

(57) Trimble, M. J.; Mlynárčik, P.; Kolář, M.; Hancock, R. E. W. Polymyxin: Alternative Mechanisms of Action and Resistance. *Cold Spring Harb Perspect Med* **2016**, *6*, a025288.

(58) Krause, K. M.; Serio, A. W.; Kane, T. R.; Connolly, L. E. Aminoglycosides: An Overview. *Cold Spring Harb Perspect Med* **2016**, *6*, a027029.

(59) Schaudinn, C.; Dittmann, C.; Jurisch, J.; Laue, M.; Günday-Türeli, N.; Blume-Peytavi, U.; Vogt, A.; Rancan, F. Development, standardization and testing of a bacterial wound infection model based on ex vivo human skin. *PLOS ONE* **2017**, *12*, e0186946.

(60) Steinstraesser, L.; Sorkin, M.; Niederbichler, A. D.; Becerikli, M.; Stupka, J.; Daigeler, A.; Kesting, M. R.; Stricker, I.; Jacobsen, F.; Schulte, M. A novel human skin chamber model to study wound infection ex vivo. *Archives of Dermatological Research* **2010**, *302*, 357-365.

(61) Yoon, D. J.; Fregoso, D. R.; Nguyen, D.; Chen, V.; Strbo, N.; Fuentes, J. J.; Tomic-Canic, M.; Crawford, R.; Pastar, I.; Isseroff, R. R. A tractable, simplified ex vivo human skin model of wound infection. *Wound Repair and Regeneration* **2019**, *27*, 421-425.

(62) Summerfield, A.; Meurens, F.; Ricklin, M. E. The immunology of the porcine skin and its value as a model for human skin. *Molecular Immunology* **2015**, *66*, 14-21.

(63) McIntyre, M. K.; Peacock, T. J.; Akers, K. S.; Burmeister, D. M. Initial Characterization of the Pig Skin Bacteriome and Its Effect on In Vitro Models of Wound Healing. *PloS one* **2016**, *11*, e0166176-e0166176.

(64) Seaton, M.; Hocking, A.; Gibran, N. S. Porcine Models of Cutaneous Wound Healing. *ILAR Journal* **2015**, *56*, 127-138.

(65) Gupta, V.; Datta, P. Next-generation strategy for treating drug resistant bacteria: Antibiotic hybrids. *The Indian journal of medical research* **2019**, *149*, 97-106.

(66) Pokrovskaya, V.; Belakhov, V.; Hainrichson, M.; Yaron, S.; Baasov, T. Design, Synthesis, and Evaluation of Novel Fluoroquinolone−Aminoglycoside Hybrid Antibiotics. *Journal of Medicinal Chemistry* **2009**, *52*, 2243-2254.

(67) Andrianov, A. K.; Chen, J.; LeGolvan, M. P. Poly(dichlorophosphazene) as a precursor for biologically active polyphosphazenes: Synthesis, characterization, and stabilization. *Macromolecules* **2004**, *37*, 414-420.

(68) Albright, V.; Selin, V.; Hlushko, H.; Palanisamy, A.; Marin, A.; Andrianov, A. K.; Sukhishvili, S. A.: Fluorinated Polyphosphazene Coatings Using Aqueous Nano-Assembly of Polyphosphazene Polyelectrolytes. In *Polyphosphazenes in Biomedicine, Engineering, and Pioneering Synthesis*; ACS Symposium Series 1298; American Chemical Society, 2018; Vol. 1298; pp 101-118.

(69) Mahjour, S. B.; Sefat, F.; Polunin, Y.; Wang, L.; Wang, H. Improved cell infiltration of electrospun nanofiber mats for layered tissue constructs. *Journal of Biomedical Materials Research Part A* **2016**, *104*, 1479-1488.

(70) Fu, X.; Xu, M.; Liu, J.; Qi, Y.; Li, S.; Wang, H. Regulation of migratory activity of human keratinocytes by topography of multiscale collagen-containing nanofibrous matrices. *Biomaterials* **2014**, *35*, 1496-1506.